Somboon Sukpancharoen
Division of Mechatronics and Robotics Engineering,
Rajamangala University of Technology Thanyaburi,
Pathum Thani 12110, Thailand
e-mail: somboon_s@rmutt.ac.th

Poj Hansirisawat
Interdisciplinary of Sustainable Energy and Resources Engineering,
Faculty of Engineering,
Kasetsart University,
50 Thanon Ngamwongwan,
Lat Yao, Chatuchak, Bangkok 10900, Thailand
e-mail: poj.h@ku.th

Thongchai R. Srinophakun[1]
Department of Chemical Engineering,
Faculty of Engineering,
Kasetsart University,
50 Thanon Ngamwongwan,
Lat Yao, Chatuchak, Bangkok 10900, Thailand
e-mail: fengtcs@ku.ac.th

Implementation of Response Surface to Optimum Biodiesel Power Plant Derived From Empty Fruit Bunch

This study examined product separation in biodiesel power plants to optimize the process. Response surface methodology (RSM) was used to identify the optimum parameters for the process of separation, to maximize profitability while also reducing carbon dioxide emissions. The mass and energy balance was assessed using ASPEN PLUS *software, while RSM was carried out with* DESIGN-EXPERT *software. Development of the characteristic equation determined that the model for gasoline yield, power generation, and carbon dioxide emissions was significant at the 95% confidence level. The R-squared value predicted by the model was found to be 0.97–1.00. In an optimal plant, profit can rise by 3836 USD over the year, while carbon dioxide emissions decline annually by 17.97 tons.*
[DOI: 10.1115/1.4050817]

Keywords: biodiesel production, empty fruit bunches, optimization, response surface methodology, Box–Behnken, energy conversion/systems, energy from biomass, renewable energy

1 Introduction

The Ministry of Energy (Thailand) has a vision to promote sustainable technology and development to mitigate the impact of climate change. The strategy aims to increase the share of electricity generation derived from a renewable resource by providing the extra price of electricity. The government aims to generate 20% of electricity from biomass, from the current level of only 9.1% [1]. To study the feasibility of operating a power plant derived from biomass, empty fruit bunches (EFBs) are selected as a case study. According to a recent report, the residue of EFBs equated to approximately 0.97 million tons in 2015 [2]. The EFBs typically contain 30–60% of cellulose, 15–35% of hemicellulose, and 4–20% of lignin on a dry weight basis [3]. These major components influence the heating value of the final fuel product, while lignin has a positive and direct linear relationship with heating value [4].

Nevertheless, biomass power plants in Thailand mostly use the direct combustion process [5]. This kind of power system is not suitable since it produces higher particulate emissions [6]. Most mitigation technologies purposely dealing with this emission of direct combustion are still under development [7]. Therefore, to efficiently produce electricity, bio-oil production is required as a suitable source of fuel feedstock. One promising conversion process for generating biofuel is fast pyrolysis [8]. Bio-oil is not, however, perceived to be of good quality because it contains high levels of sulfur and oxygen, resulting in lower heating value and a product that cannot be used in regular combustion engines [9,10]. Hence, the hydrotreatment process has been developed to upgrade the quality of bio-oil into biodiesel as a competitive biofuel for the diesel generator.

However, when developing a biodiesel power plant, by reviewing the relevant literature to fulfill the designated production requirements, there is only a single set of operating conditions. To the extent that the performance of the system can be improved through analysis, the optimization technique can be utilized by choosing several variables in a different set of conditions directly relating to the study objective. Optimization can improve the plant to obtain the best possible results [11]. Among the optimization techniques, central composite design (CCD) and Box–Behnken are in widespread use since they have the benefit of optimizing many factors with a suitable number of experimental runs [12].

The CCD and Box–Behnken optimization techniques form a part of response surface methodology (RSM). The RSM approach involves a combination of mathematical and statistical methods, serving to create an appropriate polynomial equation to fit the factors in the experiment, and explains how these factors behave within the case study context [13]. It is useful for applying to a system influenced by several variables.

Therefore, this study focuses on the optimization of biodiesel production from EFBs with the objectives of obtaining the highest profit, lowest energy consumption, and lowest CO_2 emissions. ASPEN PLUS V.8.8 software is utilized to determine the mass and energy balance throughout the process. MATLAB R2018a software is utilized to develop the diesel engine since none is built-in to ASPEN PLUS. DESIGN-EXPERT V.12.0.8 (trial) software is used to calculate the optimization level. As a result of the optimization

Table 1 Composition of EFB [14]

Elemental composition	Air-dried basis (wt%)
Carbon	43.80
Hydrogen	6.20
Oxygen	42.64
Nitrogen	0.44
Sulfur	0.09
Others	0.53
Ash	6.30
Proximate composition	
Moisture	8.34
Volatile	73.16
Ash	6.30
Fixed carbon	12.20

[1]Corresponding author.

Contributed by the Advanced Energy Systems Division of ASME for publication in the JOURNAL OF ENERGY RESOURCES TECHNOLOGY. Manuscript received August 5, 2020; final manuscript received April 5, 2021; published online May 7, 2021. Assoc. Editor: Huhyun Lee.

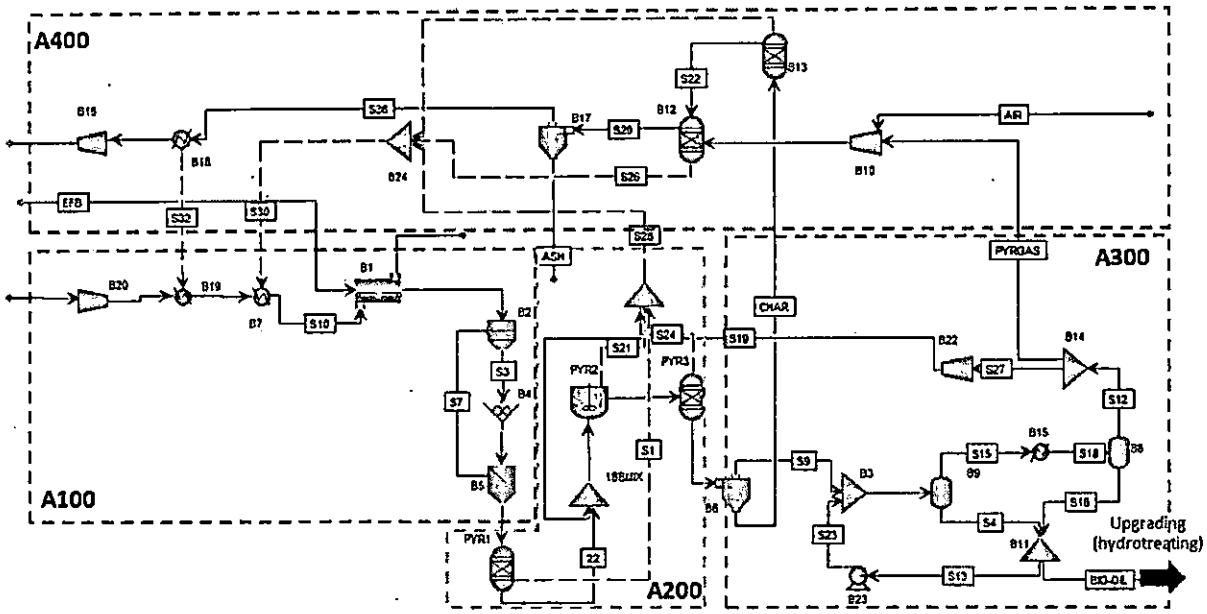

Fig. 1 Pretreatment section (A100), pyrolysis section (A200), separation section (A300), and combustion section (A400)

process, both economic and CO_2 emissions are discussed in this study.

2 Procedures

2.1 Process Modeling. The elemental composition of EFBs is as cited in the experimental research [14]. The composition of EFBs in this study is shown in Table 1. At Fig. 1, the feeding rate of EFBs is fixed at 200 kg/h. The EFBs are first transferred to the pretreatment process (A100), involving drying and crushing the EFBs to make them compatible with the fast pyrolysis process. Since the EFBs are small and have a low moisture content, the fast pyrolysis mechanism can be substantially improved to achieve the best bio-oil yield and quality. Following pretreatment, EFBs can be transferred for fast pyrolysis (A200), whereby they are decomposed to form a number of valuable products such as bio-oil, biochar, and syngas. These pyrolytic products are separated from each other in the separation system (A300). This is achieved by utilizing cyclone equipment to remove the biochar, and flash drums to condensate the bio-oil out of incondensable vapor. The byproducts are then used for heat recovery (A400) within the plant. This study assumes that the optimization process only concerns the distillation section (A600).

The bio-oil produced during the fast pyrolysis process is introduced into the hydrotreatment process. This hydrotreatment requires pure H_2 gases to remove the unwanted compounds, as mentioned in Sec. 1. The hydrotreatment process provides higher yields and improves the quality of pyrolyzed bio-oil [15]. During this process, the temperature and pressure reach 387 °C and 87 bar, respectively. After the bio-oil has been hydrotreated, it is then fed into the separation process, comprising two distillation columns. The first distillation column is used to separate the gasoline from the heavy fraction. The role of the second (diesel) column is to allow the biodiesel to be separated out of the heavy compounds. Once distillation is complete, the hydrocracking process begins to treat the remaining heavy compounds. The hydrocracking process also utilizes H_2 gas to extract some of the precious material inside the heavy compounds for recycling to the distillation process. A schematic of the upgrading section is shown in Fig. 2. The main operating conditions of the upgrading section are detailed in Table 1.

As previously mentioned, the diesel generator is developed in MATLAB. The theoretical equation is used to determine the energy output of the diesel generator according to the specific amount of biodiesel introduced.

The simple diagram in Fig. 3 represents the working cycle of an internal combustion diesel engine. At point 1, the cylinder locates at the bottom dead center (BDC), and the inlet and exhaust valves have just recently closed, with the atmospheric air already filling the entire combustion chamber. At point 2, the cylinder moves upward from BDC to top dead center (TDC) to compress all the air to create high pressure, generally raising the temperature inside the combustion chamber. In point 3, since the air has been completely pressurized, the fuel injection operates to feed the fuel into the chamber. Once the air and fuel have become completely mixed at point 3 inside the combustion chamber, the mixture ignites, rapidly expanding the chamber under a process of constant pressure. At point 4, the pressure of the burnt substances is reduced due to the general expansion of the combustion chamber as a result of the cylinder moving downward to BDC. At point 5, the combustion process is complete, with the pressure and temperature of flue gas being relatively low due to the burning mechanism. Points 6 and 7 represent the exhaust process. The exhaust valve is open and the flue gas flows out of the combustion chamber aided by the cylinder moving upward to TDC. The piston then moves down to BDC, with the inlet valve simultaneously opening to draw air from the atmosphere into the combustion chamber. This takes the combustion system back to point 1, from where it began, to carry out the diesel engine cycle once again.

Some of the equations are given as follows [16]:

$$m_{as} = \eta_v \left[\frac{P_1 V_{cyl}}{R_a T_1}\right] \tag{1}$$

$$P_2 = P_1 \left[\frac{V_{cyl}}{V_{cv}}\right]^{\gamma} \tag{2}$$

$$T_2 = \frac{P_2 V_{cv}}{m_{as} R_a} \tag{3}$$

$$W_1^2 = \frac{P_2 V_{cv} - P_1 V_{cyl}}{1 - \gamma} \tag{4}$$

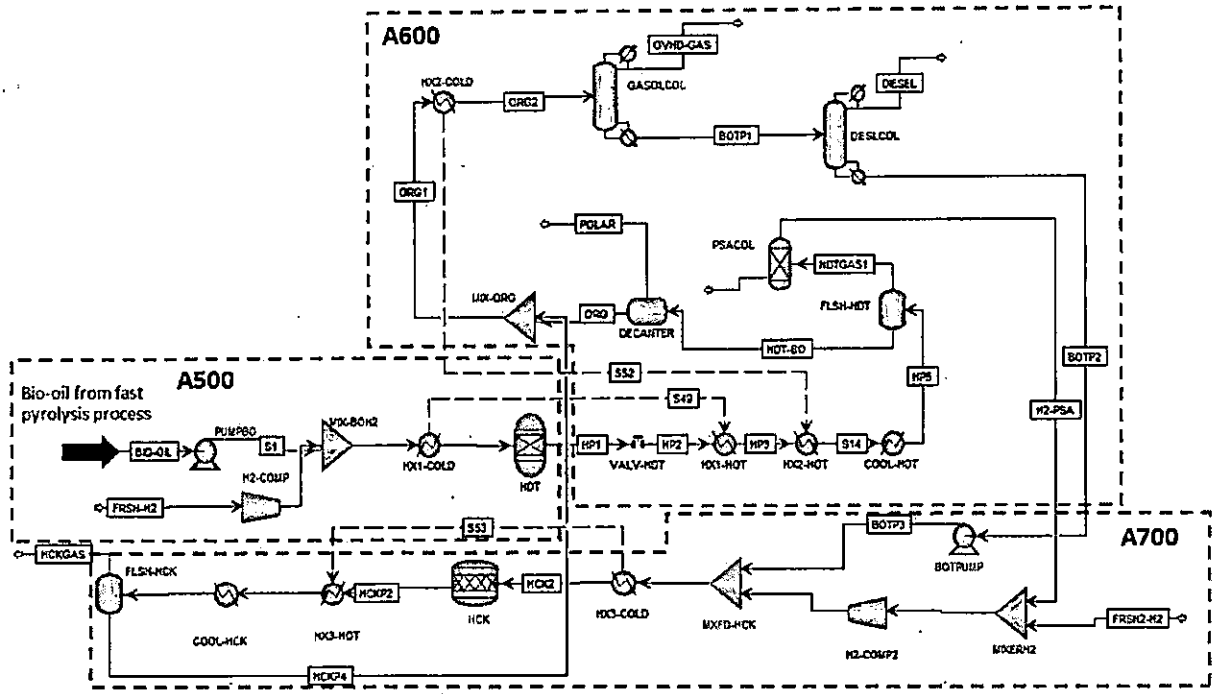

Fig. 2 Hydrotreating section (A500), distillation section (A600), and hydrocracking section (A700)

$$m_f = \frac{Q_f \times S.G.2(\text{rev/cycle})}{60.\times \text{rpm}} \tag{5}$$

$$AFR = \frac{m_{as}}{m_f} \tag{6}$$

$$\lambda = \frac{AFR}{AFR_{sto}} \tag{7}$$

$$\eta_c = 0.35332 + 0.56797\gamma - 0.12472\gamma^2 \tag{8}$$

$$Q_R = \eta_c \times C_\beta \times m_f \tag{9}$$

$$Q_2^3 = k_{cv} \times Q_R \tag{10}$$

$$T_3 = \frac{Q_2^3}{m_{as}C_v} + T_2 \tag{11}$$

$$P_3 = \frac{m_{as}R_aT_3}{V_{cv}} \tag{12}$$

$$Q_3^4 = (1 - k_{cv})Q_R \tag{13}$$

$$T_4 = \frac{Q_4^3}{m_{as}C_p} + T_3 \tag{14}$$

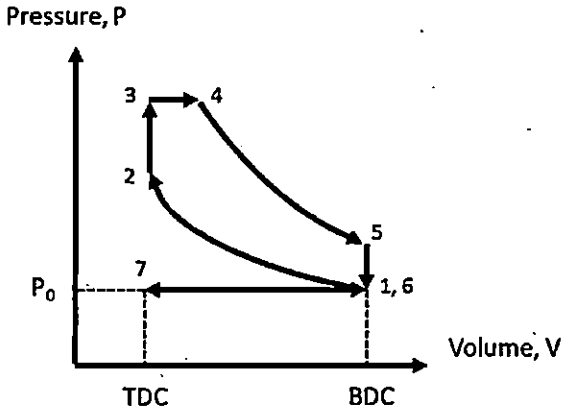

Fig. 3 Theoretical PV diagram of diesel cycle

Table 2 Important operating condition of key equipment

Sections	Key equipment	Operating conditions
Hydrotreating (A500)	Hydrotreating reactor (HDT)	Temperature: 387 °C Pressure: 87 bar
Distillation (A600)	Heat exchanger (COOL-HDT)	Temperature: 50 °C Pressure: 20 bar
	Flash drum (FLSH-HDT)	Pressure: 20 bar
	Gasoline column (GASOLCOL)	Mass reflux ratio: 1.2 [a]Mass-to-distillate ratio: 0.440 Number of stages: 9
	Diesel column (DIESLCOL)	Mass reflux ratio: 1.2 [a]Mass-to-distillate ratio: 0.897 Number of stages: 8
Hydrocracking (A700)	Hydrocracking reactor (HCK)	Temp: 670 °C Pressure: 90 bar

[a]Mass-to-distillate ratio obtained from the using of the "design spec" tool in ASPEN PLUS software. This ratio should be specified to achieve the typical distillate gasoline and biodiesel specification.

Table 3 Important specification of diesel generator

Specifications	Units	Values
Engine speed	rpm	1800
Total displacement	l	5.9
Bore × Stroke	mm × mm	102 × 120
Max. fuel consumption	l/h	30.7
Number of cylinders	–	6-inline
Compression ratio	–	17.3:1

$$V_4 = \frac{m_{as} R_a T_4}{(P_4 = P_3)} \tag{15}$$

$$W_4^3 = P_3(V_4 - V_{cv}) \tag{16}$$

$$W_4^3 = P_3(V_4 - V_{cv}) \tag{17}$$

$$P_5 = P_4\left[\frac{V_4}{V_5 = V_{cyl}}\right]^{\gamma} \tag{18}$$

$$T_5 = \frac{P_5 V_{cyl}}{m_{as} R_a} \tag{19}$$

$$W_4^5 = \frac{P_5 V_{cyl} - P_4 V_4}{1 - \gamma} \tag{20}$$

$$Q_5^6 = m_{as} C_v (T_6 - T_5) \tag{21}$$

$$W_6^7 = P_{atm}(V_{cv} - V_{cyl}) \tag{22}$$

$$W_i = W_7^1 + W_1^2 + W_3^4 + W_4^5 + W_6^7 \tag{23}$$

where η_v is the volumetric efficiency of the engine, P_1 is the pressure of atmospheric air (kPa), V_{cyl} is the volume of internal combustion cylinder (m^3), R_a is the ideal gas constant (8.31 J/(K mol)), T_1 is the temperature of atmospheric air (°C), V_{sv} is the Stroke volume (m^3), V_{cv} is the clearance volume (m^3), γ is the isentropic expansion factor, m_f is the required mass of fuel (kg), Q_f is the rate of fuel consumption (l/h), C_f is the heating value of fuel (MJ/kg), k_{cv} is the combustion performance at specific constant volume, C_v is the specific heat capacity at constant volume (J/(kg K)), and C_p is the specific heat capacity at constant pressure (J/(kg K)).

Table 4 The design matrix of the experiment

Run	Reflux ratio of GASOCOL	Temperature of COOL-HDT (°C)	Pressure of FLSH-HDT (bar)
1	0.70	60	25
2	0.70	90	15
3	1.25	90	20
4	0.15	90	20
5	0.70	60	15
6	0.70	75	20
7	1.25	60	20
8	1.25	75	15
9	0.70	90	25
10	0.15	60	20
11	0.15	75	15
12	0.15	75	25
13	1.25	75	25
14	0.70	75	20

Table 5 Economic assumptions

Economic items	Value	Ref.
[a]Operation duration (h/year)	6000	[22]
Pricé of EFB (USD/ton)	15.30	[23]
Electricity cost (USD/unit)	0.11	[24]
Operation and Maintenance cost (O&M)		[25]
Fixed O&M (USD/year)	3480	
Variable O&M (USD/MWh)	0.97	
Labor cost		
Number of workers (person)	13.791 $(MWe)^{0.4328}$	[26]
Wage of worker (USD/person/day)	10.5	[27]
Gasoline selling price (USD/l)	0.74	[28]
[b]Electricity income (USD/unit)	0.185	[29]

[a]This was made as to the assumption of the estimated total operating hour per year.
[b]This electricity income is calculated based on the consideration as this power plant is a renewable technology, Feed-in Tariffs. Thai government provides a special price for any power generation that coming from renewable sources.

According to the above theoretical equations, many specifications relate to the geometry and properties of the diesel generator. In this case, some diesel generator specifications are used to calculate the equations. The specification details are provided by selecting a diesel generator that is available in Thailand, as shown in Tables 2 and 3.

2.2 Design of Experiments. In the initial designated operating condition, the parameters might not provide the best conditions for achieving the defined objective. Hence, optimization aims to accomplish the best design, according to a set of specific conditions or constraints. These include maximizing factors such as the rate of production, benefit point, reliability, efficiency, and utilization [17]. The objectives of this study should be assessed accordingly. The power plant under study should maximize its profitability to achieve financial satisfaction. The objectives of optimizing gasoline yield and increasing the magnitude of electricity generation should then be achieved as a consequence of higher biodiesel yield. To achieve profit maximization at the plant, it is important to take utility costs into account. Since the operation of the plant involves

Table 6 Experimental matrix of Box–Behnken design with defined response values

	Level of factors employed			Responses			
Run no.	A (–)	B (°C)	C (bar)	Y_1 (kW)	Y_2 (kg/h)	Y_3 (USD/h)	Y_4 (kg/h)
1	0.70	60	25	105.99	18.38	31.123	139.31
2	0.70	90	15	100.65	19.57	30.700	137.42
3	1.25	90	20	102.00	19.33	30.858	138.13
4	0.15	90	20	102.18	19.35	30.602	136.98
5	0.70	60	15	103.81	19.70	31.070	139.08
6	0.70	75	20	103.78	19.31	30.916	138.39
7	1.25	60	20	105.02	19.03	31.227	139.78
8	1.25	75	15	102.49	19.75	31.020	138.85
9	0.70	90	25	103.38	18.96	30.748	137.63
10	0.15	60	20	104.99	19.06	30.981	138.68
11	0.15	75	15	102.45	19.78	30.767	137.72
12	0.15	75	25	104.77	18.78	30.818	137.95
13	1.25	75	25	104.77	18.78	31.070	139.07
14	0.70	75	20	103.79	19.31	30.917	138.39

Note: A, reflux ratio of GASOCOL; B, temperature of COOL-HDT (°C); C, pressure of FLSH-HDT (bar); Y_1, electricity generation (kW); Y_2, mass flowrate of gasoline (kg/h); Y_3, utility cost (USD/h); and Y_4, CO_2 emission (kg/h).

Table 7 Analysis of variance (ANOVA) of linear, quadratic, and interactive terms of the biodiesel power plant on responses (*P*-value)

Items	Electricity generation (kW)	Mass flowrate of gasoline (kg/h)	Utility cost (USD/h)	CO_2 emission (kg/h)
Model	<0.001[a]	<0.001[a]	<0.001[a]	<0.001[a]
A—reflux ratio of distillation column	0.560	0.334	<0.001[a]	<0.001[a]
B—temperature of heat exchanger	<0.001[a]	0.001[a]	<0.001[a]	<0.001[a]
C—pressure flash drum	<0.001[a]	<0.001[a]	<0.001[a]	<0.001[a]
A*B	0.218	0.875	0.001[a]	0.001[a]
A*C	0.842	0.655	0.653	0.648
B*C	0.014[a]	<0.001[a]	0.034[a]	0.033[a]
A*A	0.354	0.845	<0.001[a]	<0.001[a]
B*B	0.006[a]	<0.001[a]	<0.001[a]	<0.001[a]
C*C	0.024[a]	0.058	0.003[a]	0.003[a]
R^2	0.994	0.999	1.000	1.000

[a]Significant.

renewable technology, it is also necessary to consider carbon dioxide emissions. Therefore, this study has four objectives: (1) electricity generation (kW), (2) mass yield of gasoline, (3) utility cost, and (4) CO_2 emissions.

In terms of the dependent variable or varying factors, it is important to perform sensitivity analysis on these factors according to the objectives. In the existing literature, it is often argued that the main proportion of energy consumption in the type of plant under study will come from the distillation column, accounting for around half the total [18]. Therefore, the distillation column is an important aspect on which to focus. Many parameters potentially impact the ability of distillation in the column, such as operating pressure, reflux ratio, number of stages, and product specifications [19]. To match the distillation column specification, the reflux ratio is selected as one of the variables. The other two variables are the pressure of the flash drum (FLSH-HDT) and temperature of the heat exchanger (COOL-HDT). These two devices initially separate the light hydrocarbons (C1–C4) and H_2 gas from the hydrotreated stream. Light hydrocarbons have an extremely low boiling point with an average value lower than 5 °C [20]. These light hydrocarbons are more toxic than heavy hydrocarbons [21]. Apart from the independent factors, the other parameters are assumed to have a constant value.

After specifying the independent factors, the levels were entered into the DESIGN-EXPERT 12.0.8 (trial), and the experimental design matrix given, as shown in Table 4. According to the methodology used, 14 runs were obtained, using a randomized subtype, Box–Behnken design, and a quadratic model.

2.3 Economic Parameters. From the economic perspective, consideration should be given to the operating conditions and the setting of clear boundaries set. The only boundary requiring consideration in this study is the operating phase, with the capital cost excluded from the calculation. The economic assumptions are shown in Table 5.

3 Results and Discussion

3.1 Optimization Process. For the Box–Behnken design, a total of 14 experimental runs for formulation are proposed by the DESIGN-EXPERT software, focusing on three factors: the reflux ratio of gasoline column (A), temperature of the heat exchanger [COOL-HDT] (B), and pressure of the flash drums [FLSH-HDT] (C). These factors could be varied at three levels. The various effects of the independent factors on the generation of electricity are then examined, based on the properties of biodiesel (kW), plant utility costs (USD/h), gasoline mass yield (kg/h), and level of carbon dioxide emissions, for parameter optimization. The expected values for the planned experiment, along with the recorded responses, are presented in Table 6.

According to Table 6, it can be observed that the set of independent factors are the same for both experiments 6 and 14. It is possible to ignore these particular experiment sets to achieve a more concise optimization process. The set of responses are used to develop the polynomial equation as a representative system model. The polynomial equations are presented as a relation between the independent factors and defined objectives of this study.

The developed equation is analyzed as a representative model of the system. The results of the analysis are shown in Table 7. It can be observed that if the *P*-value of any factor is lower than the significance level of 0.05, the factor can be considered significant with a confidence level of 95%. The model of electricity generation, mass flowrate of gasoline, utility cost, and CO_2 emissions are revealed to be significant with predicted *R*-squared values of 0.9902, 0.9799, 0.9999, and 0.9999, respectively.

The model proposes the following polynomial equations for electricity generation (Y_1), mass yield of gasoline (Y_2), utility cost (Y_3), and CO_2 emissions (Y_4), respectively

$$Y_1 = 101.55556 + 0.63864A + 0.00412B + 0.31133C - 0.00582AB - 0.00255AC + 0.00181BC - 0.12727A^2 - 0.00089B^2 - 0.0052C^2 \quad (24)$$

$$Y_2 = 20.6308 - 0.0989A + 0.0402B - 0.2131C + 0.0003AB + 0.0023AC + 0.0023BC + 0.0101A^2 - 0.0005B^2 - 0.0015C^2 \quad (25)$$

$$Y_3 = 31.45617 + 0.18484A - 0.00986B + 0.01011C + 0.0032AB - 0.0006AC - 0.00001BC + 0.01487A^2 - 0.00002B^2 - 0.0001C^2 \quad (26)$$

$$Y_4 = 140.8185 + 0.82562A - 0.04436B + 0.04467C + 0.00144AB - 0.0027AC - 0.00006BC + 0.067778A^2 - 0.00007B^2 - 0.00043C^2 \quad (27)$$

A linear graph plot of the responses, as a result of varying the independent factors, is shown in Fig. 4, denoting the comparison between predicted and simulation values of electricity generation, the mass flowrate of gasoline, utility cost, and CO_2 emissions by Y_1, Y_2, Y_3, and Y_4, respectively. It can be observed that the developed linear correlation fits well with the actual value.

Details of the suggested conditions for each independent factor contributing to the optimum value of the specified criteria, along with the constraints, are presented in Table 8. It can be observed that the predicted values are not significantly different from the actual values. The percentage errors for electricity generation, yield of gasoline, utility cost, and CO_2 emissions are 0.012, 0.028, 0.007, and 0.006%, respectively. A three-dimensional response graph is appropriate for studying the related effects of the independent factors on the designed responses, as shown in Fig. 5.

The increase in pressure (15–25 bar) illustrates the rising electricity generation (100.66–105.99 kW) resulting from the higher biodiesel yield (Fig. 5(*a*)). However, the rising temperature (60–90 °C) gives the opposite result in that it decreases the magnitude

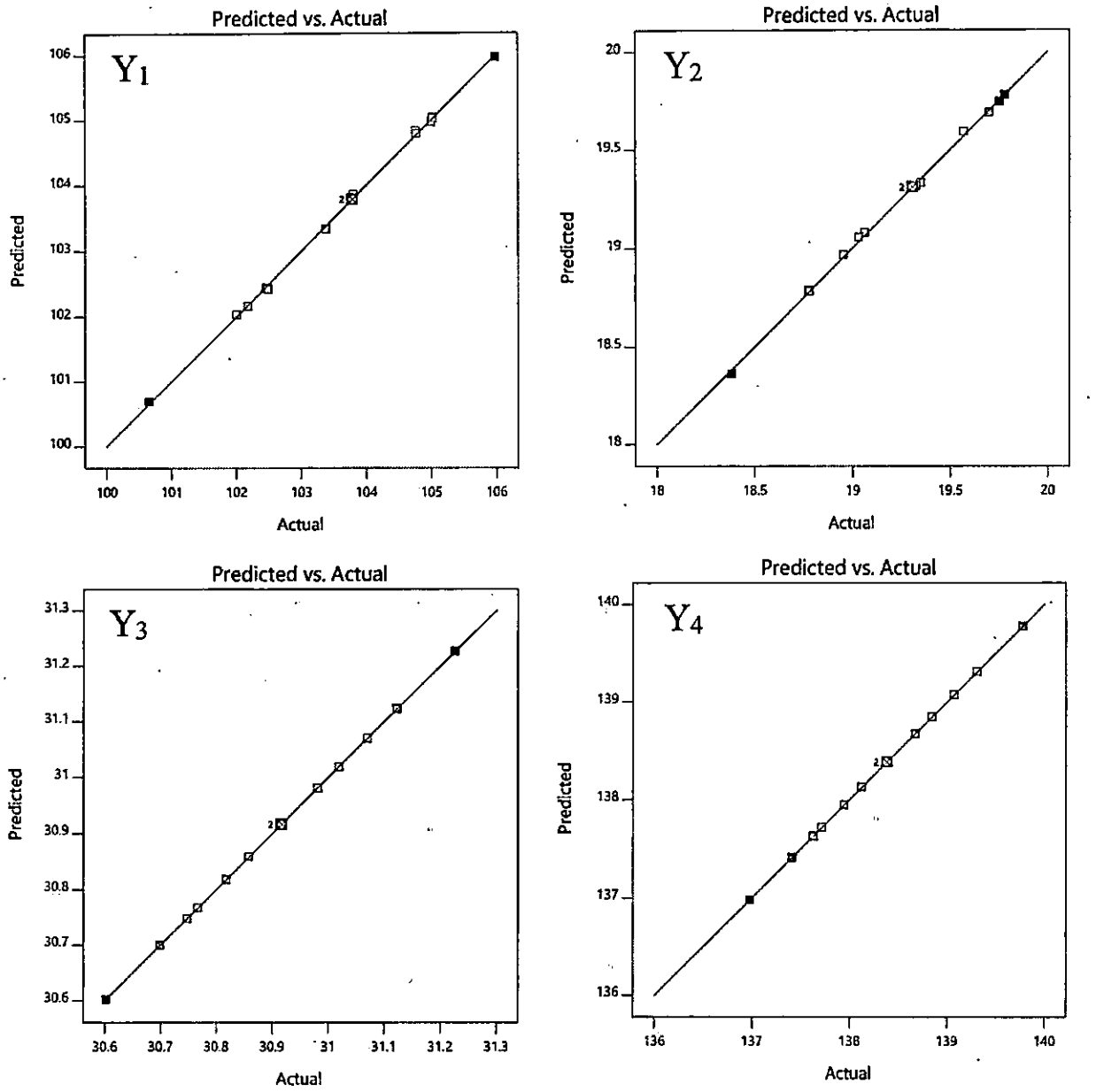

Fig. 4 Linear correlation plot between the simulation and predicted response

of electricity generation. This might be due to the higher vaporization of hydrocarbon compounds. The decrease in pressure (25–15 bar) in Fig. 5(*b*) causes an increase in the mass yield of gasoline (18.39–19.78 kg/h)—the rise in temperature creating an increasing trend in gasoline yield. The highest possible value generated for gasoline yield (19.78 kg/h) can be achieved at a temperature of 75 °C and a pressure of 15 bar. The decrease in reflux ratio (1.25–0.15) in Fig. 5(*c*) favors lower utility costs (31.23–30.60 USD/h) due to correspondingly lower energy consumption [30]. In terms of the temperature in the heat exchanger, when it is increased (60–90 °C), the utility cost decreases. The heat exchanger is responsible for heating the bio-oil to improve the separation process in the flash drum. When it reaches the optimum temperature, greater extraction of lighter hydrocarbon can be achieved. Consequently, higher the temperatures, lower the feeding rate of the distillation column, thereby reducing the effort required by the equipment. The relationship between CO_2 emissions, temperature, and pressure is examined, as shown in Fig. 5(*d*). This gives a similar result to the response surface of the utility cost. An increase in temperature (60–90 °C) raises the CO_2 emissions, while a decrease in pressure lowers the CO_2 emissions.

3.2 Economic Analysis. Besides the optimum solution (scenario 1 in Table 9) suggested by the software, other alternative solutions can be considered for economic analysis, as shown in Table 10. These scenarios offer various advantages such as increased production capacity, economic profitability, and reduced CO_2 emissions.

Table 8 shows that three different situations can provide varying responses. In scenario 2, the utility cost (30.615 USD/h) and carbon dioxide emissions (137.04 kg/h) are both at the lowest levels among all sets of responses. Scenario 3 provides the highest electricity generation of 103.38 kW among all sets of responses, while scenario 4 provides the highest gasoline production yield (19.78 kg/h) but the lowest value for electricity generation (102.71 kW). These three

Table 8 Comparison of predicted value as a result of optimizations with actual response values from the simulation

Constraints (independent factors)	Target (importance)	Experimental range	Optimal value	
Independent factors				
Reflux ratio	In range	0.15–1.25	0.15	
The temperature of COOL-HDT (°C)	In range	60–90	85.17	
Pressure of FLSH-HDT (bar)	In range	15–25	21.07	
Responses			Predicted value	Actual value
Electricity generation (kW)	Maximize	100.65–105.99	102.99	102.98
Mass yield of gasoline (kg/h)	Maximize	18.38–19.78	19.27	19.27
Utility cost (USD/h)	Minimize	30.602–31.227	30.673	30.672
CO_2 emission (kg/h)	Minimize	136.98–139.78	137.29	137.28

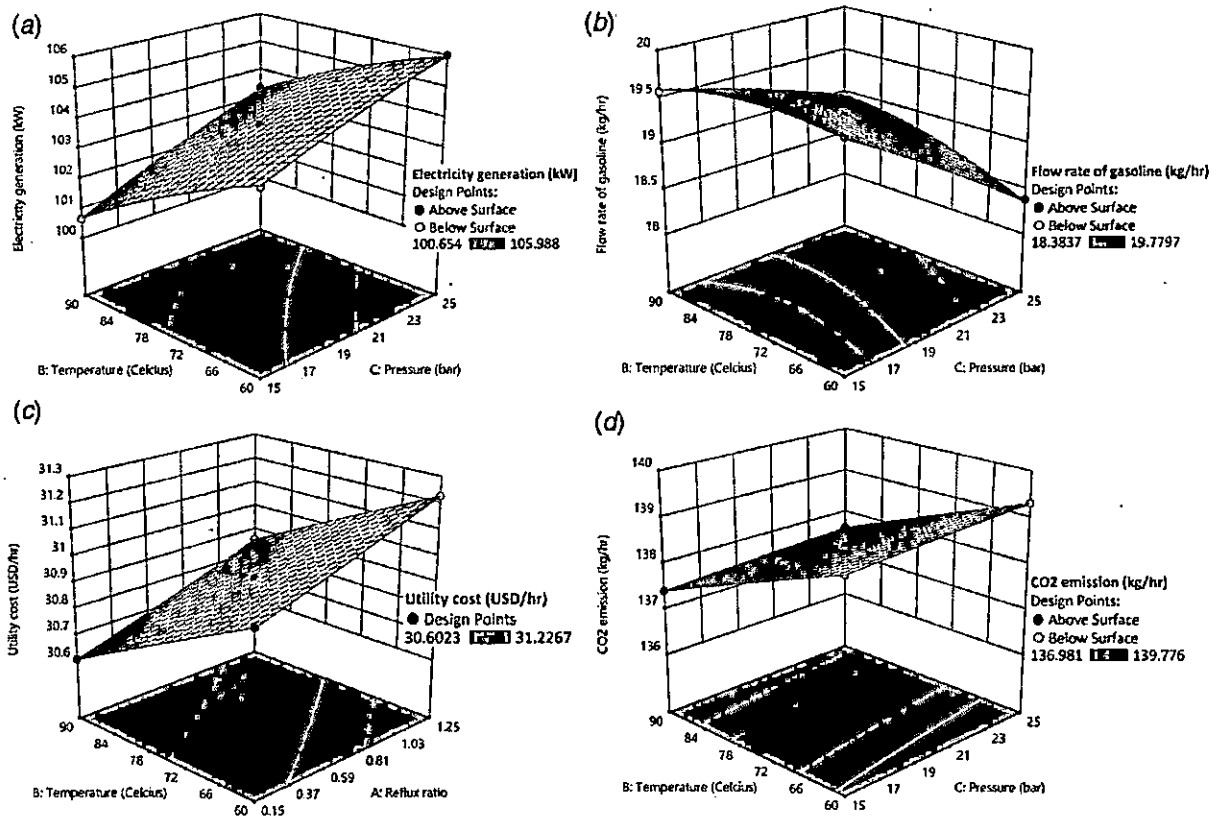

Fig. 5 (a) Effect of temperature of COOL-HDT and pressure of FLSH-HDT on electricity generation, (b) effect of temperature of COOL-HDT and pressure of FLSH-HDT on the mass yield of gasoline, (c) effect of temperature of COOL-HDT and reflux ratio of GASOCOL on utility cost, and (d) effect of temperature of COOL-HDT and pressure of FLSH-HDT on CO_2 emission

response sets will be used for further analysis from the economic perspective. The economic assumptions and method of calculation are already provided in Table 4.

The responses of these scenarios can be used to calculate the utility cost, electricity sale price, gasoline sale price, and the magnitude of CO_2 emissions. Details of both the base case, which is the original plant without the benefit of optimization, and the scenarios, with the advantage of optimization, are presented in Table 9.

The results of economic analysis and CO_2 emissions are shown in Fig. 6. It is clear that in scenario 4, where the highest level of

Table 9 The alternative scenarios of the responses

Scenarios	Reflux ratio of distillation column	Temperature of heat exchanger (°C)	Pressure of flash drum (bar)	Electricity generation (kW)	Yield of gasoline (kg/h)	Utility cost (USD/year)	CO_2 emission (kg/h)
1 (optimum value)	0.15	85.17	21.07	102.99	19.27	30.67	137.29
2	0.15	90.00	22.75	102.85	19.14	30.62	137.04
3	0.15	82.64	21.58	103.38	19.22	30.71	137.44
4	0.15	72.51	15.07	102.71	19.78	30.80	137.86

Table 10 Economic comparison between the scenarios and the base case

	Scenarios				
	Base case	1 (optimum condition)	2	3	4
Cost (USD/year)					
EFB feed stock	18,360	18,360	18,360	18,360	18,360
Utility cost	188,037	184,020	183,690	184,230	184,794
Fixed O&M	3480	3480	3480	3480	3480
Variable O&M	616	599	599	602	598
Wage of labour	16,443	16,443	16,443	16,443	16,443
Income (USD/year)					
Power generation	117,451	114,319	114,167	114,756	114,004
Gasoline	111,219	114,154	113,396	113,876	117,152
Profit (USD/year)	1735	5571	4991	5518	7481
Environment					
CO_2 emission (tons CO_2/year)	842	824	822	825	827

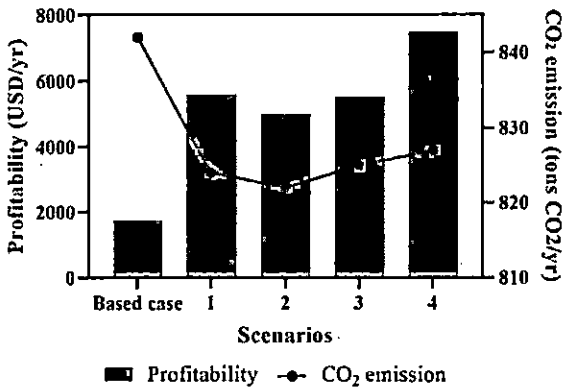

Fig. 6 Profitability and CO_2 emission of each scenarios

gasoline production and maximum profitability of 7481 USD/year can be achieved, carbon dioxide emissions are also the highest recorded at 827 tons/year. In scenario 2, these independent variable sets can offer the best performance for an environmentally friendly power plant, producing just 822 tons of CO_2/year in emissions. However, in economic terms, it contributed the smallest profit of all scenarios. To fulfill both economic and environmental requirements, the scenario suggested by the DESIGN-EXPERT might be the optimum response (scenario 1) since the profit is almost the highest at 5571 USD/year, with the CO_2 emissions almost the lowest at 824 tons CO_2/year, among all scenarios. However, the choice of suitable factors for successful operation will be dependent upon the power plant objectives. If the project owner considers profitability to be a priority, scenario 4 might be the most suitable option. However, if the owner wishes to focus on the environmental issue, scenario 2 is the best option for sustainable technology utilization. In order to propose the designed model, a modern technology called deep learning [31,32] can be implemented. This will help investors to make decision while introducing into a smart grid.

4 Conclusion

This study examines the use of EFBs for generating electrical power. The efficient production of electricity requires EFBs to first undergo conversion into biofuel. The power plant then uses a fast pyrolysis process for the conversion. However, in optimizing the operation of the power plant, the environmental impact and economic outcomes cannot be ignored. For this reason, RSM is employed in the optimization process. The simulation findings reveal that in the initial base condition with no optimization, the following results were achieved for power generation (105.81 kW), gasoline mass yield (18.78 kg/h), utility cost (31.34 USD/h), and carbon dioxide emissions (140.28 kg/h). The optimization using DESIGN-EXPERT V.12.0.8 (trial) software proposed the optimum point for the reflux ratio of GASOCOL at 0.15, while the temperature of COOL-HDT should be 85.17 °C, with the FLSH-HDT pressure at 21.07 bar. With the independent factors optimized, the following results were reported for power generation (102.99 kW), gasoline mass yield (19.27 kg/h), utility cost (30.67 USD/h), and carbon dioxide emissions (137.29 kg/h). The outcome in terms of profit was an annual increase of 3836 USD, while carbon dioxide emissions declined by 17.97 tons annually. Although this scenario is optimized from the economic and environmental perspective, an alternative exists which would maximize profitability but, unfortunately, also yield the highest carbon dioxide emissions. Meanwhile, another choice offers superior environmental performance but minimizes profit. In this case, the decision must fall to the owner of the plant, who must decide which scenario to favor, according to the objectives of the business. In any event, the optimized approach will be superior to the non-optimized alternatives.

This work's limitation is that the biodiesel power plant model developed on ASPEN PLUS software might not be entirely and perfectly validated because of the lack of an actual prototype of the plant utilized to reference results. Recently, the problem of EFB in terms of the environment has been widely concerned. Many institutions try many different ways to utilize the EFB as material for the commercialized product properly. Fast pyrolysis is one of the promising technologies. The full cycle of operation utilized the fast pyrolysis, as a core bioconversion process, has not completely developed. The future of the present work might be further analysis on the uncertainty of the individual process. The improvement in economic assessment might be required to achieve more on the accuracy of profitability evaluation.

Acknowledgment

This work was supported the computer device and working place by Rajamangala University of Technology (RMUTT) Thailand. This research is supported by the Thailand Advanced Institute of Science and Technology and Tokyo Institute of Technology (TAIST-Tokyo Tech) program under the National Science and Technology Development Agency (NSTDA). This research was also supported by grants funded by the National Research Council of Thailand (NRCT) and the Research University Network.

Conflict of Interest

There are no conflicts of interest.

References

[1] Sutabutr, T., 2012, "Alternative Energy Development Plan: AEDP 2012–2021," J. Renew. Energy Smart Grid Technol., 7(1), pp. 1–10.

[2] Chanlongphitak, S., Papong, S., Malakul, P., and Mungcharoen, T., 2015, "Life Cycle Assessment of Palm Empty Fruit Bunch Utilization for Power Plants in Thailand," International Conference on Biological, Environment and Food Engineering, Singapore, May 15–16, Vol. 515048.

[3] Choojit, S., and Sangwichien, C., 2018, "Preparation of Activated Carbon Production From Oil Palm Empty Fruit Bunch and Its Application," Kasem Bundit Eng. J., 8(2), pp. 48–67.

[4] Mansora, A. M., Lima, J. S., Anib, F. N., Hashima, H., and Hoa, W. S., 2019, "Characteristics of Cellulose, Hemicellulose, and Lignin of MD2 Pineapple Biomass," Chem. Eng., 72(1), p. 79–84.

[5] Barz, M., and Delivand, M. K., 2011, "Agricultural Residues as Promising Biofuels for Biomass Power Generation in Thailand," J. Sustain. Energy Environ. Special Issue, 21(1), pp. 27.

[6] Riva, G., Pedretti, E. F., Toscano, G., Duca, D., and Pizzi, A., 2011, "Determination of Polycyclic Aromatic Hydrocarbons in Domestic Pellet Stove Emissions," Biomass Bioenergy, 35(10), pp. 4261–4267.

[7] Lim, M. T., Phan, A., Roddy, D., and Harvey, A., 2015, "Technologies for Measurement and Mitigation of Particulate Emissions From Domestic Combustion of Biomass: A Review," Renew. Sustain. Energy Rev., 49(1), pp. 574–584.

[8] Pattiya, A., Titiloye, J. O., and Bridgwater, A. V., 2009, "Fast Pyrolysis of Agricultural Residues From Cassava Plantation for Bio-Oil Production," Carbon, 51(1), pp. 51–59.

[9] Xu, Y., Hu, X., Li, W., and Shi, Y., 2011, *Preparation and Characterization of Bio-Oil From Biomass*, InTech Publisher, Rijeka, Croatia, pp. 197–222.

[10] Zheng, J. L., and Wei, Q., 2011, "Improving the Quality of Fast Pyrolysis Bio-Oil by Reduced Pressure Distillation," Biomass Bioenergy, 35(5), pp. 1804–1810.

[11] Araujo, P. W., and Brereton, R. G., 1996, "Experimental Design I. Screening," TrAC Trends Anal. Chem., 15(1), pp. 26–31.

[12] Asghar, A., Abdul Raman, A. A., and Daud, W. M. A. W., 2014, "A Comparison of Central Composite Design and Taguchi Method for Optimizing Fenton Process," Sci. World J., 2014(1), pp. 1–14.

[13] Bezerra, M. A., Santelli, R. E., Oliveira, E. P., Villar, L. S., and Escaleira, L. A., 2008, "Response Surface Methodology (RSM) as a Tool for Optimization in Analytical Chemistry," Talanta, 76(5), pp. 965–977.

[14] Kerdsuwan, S., and Laohalidanond, K., 2011, "Renewable Energy From Palm Oil Empty Fruit Bunch," Renew. Energy-Trends Appl., pp. 123–150.

[15] Auersvald, M., Shumeiko, B., Vrtiška, D., Straka, P., Staš, M., Šimáček, P., Blažek, J., and Kubička, D., 2019, "Hydrotreatment of Straw Bio-Oil From Ablative Fast Pyrolysis to Produce Suitable Refinery Intermediates," Fuel, 238(1), pp. 98–110.

[16] Vathakit, K., 2012, "A Study of Boost Pressure on Efficiency of an Agricultural Single Cylinder Diesel Engine—Theory and Calculations," TSAE International Conference, Chiang Mai, Apr. 4–5.

[17] Merrill, C., Custer, R. L., Daugherty, J. L., Westrick, M., and Zeng, Y., 2008, "Delivering Core Engineering Concepts to Secondary Level Students," J. Technol. Edu., 20(1).

[18] Lee, J., Son, Y., Lee, K. S., and Won, W., 2019, "Economic Analysis and Environmental Impact Assessment of Heat Pump-Assisted Distillation in a Gas Fractionation Unit," Energies, 12(5), p. 852.

[19] Cui, C., Liu, S., and Sun, J., 2018, "Optimal Selection of Operating Pressure for Distillation Columns," Chem. Eng. Res. Des., 137(1), pp. 291–307.

[20] Group, T.P.H.T., 2009, Report from https://www.petroleumhpv.org/petroleum-substances-and-categories/~/media/9540E567AE1A4D69833DE465ECCF3D02.ashx.

[21] Labud, V., Garcia, C., and Hernandez, T., 2007, "Effect of Hydrocarbon Pollution on the Microbial Properties of a Sandy and a Clay Soil," Chemosphere, 66(10), pp. 1863–1871.

[22] Delivand, M. K., Barz, M., and Gheewala, S. H., 2011, "Logistics Cost Analysis of Rice Straw for Biomass Power Generation in Thailand," Energy, 36(3), pp. 1435–1441.

[23] (EforE), E.f.E.F., Report from Department of Alternative Energy Development and Efficiency Thailand, http://webkc.dede.go.th/testmax/sites/default/files/%E0%B8%90%E0%B8%B2%E0%B8%99%E0%B8%82%E0%B9%89%E0%B8%AD%E0%B8%A1%E0%B8%B9%E0%B8%A5%E0%B8%81%E0%B8%B2%E0%B8%A3%E0%B8%A5%E0%B8%87%E0%B8%97%E0%B8%B8%E0%B8%99%E0%B8%9C%E0%B8%A5%E0%B8%B4%E0%B8%95%E0%B8%9E%E0%B8%A5%E0%B8%B1%E0%B8%87%E0%B8%87%E0%B8%B2%E0%B8%99%E0%B9%84%E0%B8%9F%E0%B8%9F%E0%B9%89%E0%B8%B2%E0%B8%88%E0%B8%B2%E0%B8%81%E0%B8%97%E0%B8%B0%E0%B8%A5%E0%B8%B2%E0%B8%A2%E0%B8%9B%E0%B8%B2%E0%B8%A5%E0%B9%8C%E0%B8%A1%E0%B9%80%E0%B8%9B%E0%B8%A5%E0%B9%88%E0%B8%B2_0.pdf.

[24] (MEA), M.E.A, 2018 Medium General Service of Electricity (Applicability). https://www.mea.or.th/download/view/26327, Accessed April 27, 2020.

[25] Promjiraprawat, K., and Limmeechokchai, B., 2013, "Multi-Objective and Multi-Criteria Optimization for Power Generation Expansion Planning With CO_2 Mitigation in Thailand," Songklanakarin J. Sci. Technol., 35(3), pp. 349–359.

[26] Delivand, M. K., Barz, M., Gheewala, S. H., and Sajjakulnukit, B., 2011, "Economic Feasibility Assessment of Rice Straw Utilization for Electricity Generating Through Combustion in Thailand," Appl. Energy, 88(11), pp. 3651–3658.

[27] Labour, M.o. Minimum Wage. 1 January 2020, https://www.mol.go.th/en/minimum-wage/.

[28] Thailand Gasoline Prices, 2020. https://www.globalpetrolprices.com/Thailand/gasoline_prices/, Accessed March 30, 2020.

[29] Tantisattayakul, T., and Kanchanapiya, P., 2017, "Financial Measures for Promoting Residential Rooftop Photovoltaics Under a Feed-In Tariff Framework in Thailand," Energy Policy, 109(1), pp. 260–269.

[30] De Figueiredo, M. F., Brito, K. D., Ramos, W. B., Sales Vasconcelos, L. G., and Brito, R. P., 2015, "Effect of Solvent Content on the Separation and the Energy Consumption of Extractive Distillation Columns," Chem. Eng. Commun., 202(9), pp. 1191–1199.

[31] Prabadevi, B., Quoc-Viet, P., Madhusanka, L., Deepa, N., Mounik, V. V. S. S., Shivani, R., Praveen, K. R. M., Neelu, K., Thippa, R. G., and Won-Joo, H., 2021, "Deep Learning for Intelligent Demand Response and Smart Grids: A Comprehensive Survey," Comput. Sci.

[32] Alazab, M., Khan, S., Krishnan, S. S. R., Pham, Q. V., Praveen Kumar Reddy, M., and Gadekallu, T. R., 2020, "A Multidirectional LSTM Model for Predicting the Stability of a Smart Grid," IEEE Access, 8(1), pp. 85454–85463.

Journal of Energy Resources Technology. Received August 05, 2020;
Accepted manuscript posted April 05, 2021. doi:10.1115/1.4050817

IMPLEMENTATION OF RESPONSE SURFACE METHODOLOGY TO CREATE AN OPTIMUM BIODIESEL POWER PLANT DERIVED FROM EMPTY FRUIT BUNCHES

Somboon Sukpancharoen
Division of Mechatronics and Robotics Engineering, Rajamangala University of Technology Thanyaburi, Pathum Thani 12110, Thailand
somboon_s@rmutt.ac.th

Poj Hansirisawat
Interdisciplinary of Sustainable Energy and Resources Engineering, Faculty of Engineering, Kasetsart University 50 Thanon Ngamwongwan, Lat Yao, Chatuchak, Bangkok 10900, Thailand
poj.h@ku.th

Thongchai R. Srinophakun[1]
Department of Chemical Engineering, Faculty of Engineering, Kasetsart University 50 Thanon Ngamwongwan, Lat Yao, Chatuchak, Bangkok 10900, Thailand
fengtcs@hotmail.com

[1] Corresponding author

ABSTRACT

This study examined product separation in biodiesel power plants to optimise the process. Response Surface Methodology (RSM) was used to identify the optimum parameters for the process of separation, to maximise profitability while also reducing carbon dioxide emissions. The mass and energy balance was assessed using Aspen Plus software, while RSM was carried out with Design-Expert software. Development of the characteristic equation determined that the model for gasoline yield, power generation, and carbon dioxide emissions was significant at the 95% confidence level. The R-squared value predicted by the model was found to be 0.97–1.00. In an optimal plant, profit can rise by 3,836 USD over the year, while carbon dioxide emissions decline annually by 17.97 tons.

Keywords: *Biodiesel production, Empty fruit bunches, Optimisation, Response surface methodology, Box-Behnken*

Journal of Energy Resources Technology. Received August 05, 2020;
Accepted manuscript posted April 05, 2021. doi:10.1115/1.4050817

1 Introduction

The Ministry of Energy (Thailand) has a vision to promote sustainable technology and development to mitigate the impact of climate change. The strategy aims to increase the share of electricity generation derived from a renewable resource by providing the extra price of electricity. The government aims to generate 20% of electricity from biomass, from the current level of only 9.1% [1]. To study the feasibility of operating a power plant derived from biomass, empty fruit bunches (EFBs) are selected as a case study. According to a recent report, the residue of EFBs equated to approximately 0.97 million tons in 2015 [2]. The EFBs typically contain 30–60% of cellulose, 15–35% of hemicellulose, and 4–20% of lignin on a dry weight basis [3]. These major components influence the heating value of the final fuel product, while lignin has a positive and direct linear relationship with heating value [4].

Nevertheless, biomass power plants in Thailand mostly use the direct combustion process [5]. This kind of power system is not suitable since it produces higher particulate emissions [6]. Most mitigation technologies purposely dealing with this emission of direct combustion are still under development [7]. Therefore, to efficiently produce electricity, bio-oil production is required as a suitable source of fuel feedstock. One promising conversion process for generating biofuel is fast pyrolysis [8]. Bio-oil is not, however, perceived to be of good quality because it contains high levels of sulphur and oxygen, resulting in lower heating value and a product that cannot be used in regular combustion engines [9, 10]. Hence, the hydrotreatment process has been developed to

Journal of Energy Resources Technology. Received August 05, 2020;
Accepted manuscript posted April 05, 2021. doi:10.1115/1.4050817

upgrade the quality of bio-oil into biodiesel as a competitive biofuel for the diesel generator.

However, when developing a biodiesel power plant, by reviewing the relevant literature to fulfil the designated production requirements, there is only a single set of operating conditions. To the extent that the performance of the system can be improved through analysis, the optimisation technique can be utilised by choosing several variables in a different set of conditions directly relating to the study objective. Optimisation can improve the plant to obtain the best possible results [11]. Among the optimisation techniques, Central Composite Design (CCD) and Box-Behnken are in widespread use since they have the benefit of optimising many factors with a suitable number of experimental runs [12].

The CCD and Box-Behnken optimisation techniques form part of Response Surface Methodology (RSM). The RSM approach involves a combination of mathematical and statistical methods, serving to create an appropriate polynomial equation to fit the factors in the experiment, and explain how these factors behave within the case study context [13]. It is useful for applying to a system influenced by several variables.

Therefore, this study focuses on the optimisation of biodiesel production from EFBs with the objectives of obtaining the highest profit, lowest energy consumption, and lowest CO_2 emissions. Aspen Plus V.8.8 software is utilised to determine the mass and energy balance throughout the process. MATLAB R2018a software is utilised to develop the diesel engine since none is built-in to Aspen Plus. Design-Expert V.12.0.8 (trial)

Journal of Energy Resources Technology. Received August 05, 2020;
Accepted manuscript posted April 05, 2021. doi:10.1115/1.4050817

software is used to calculate the optimisation level. As a result of the optimisation process, both economic and CO_2 emissions are discussed in this study.

2 Procedures

2.1 Process modelling

The elemental composition of EFBs is as cited in the experimental research [14]. The composition of EFBs in this study is shown in Table 1. At Fig. 1, the feeding rate of EFBs is fixed at 200 kg/hr. The EFBs are firstly transferred to the pretreatment process (A100), involving drying and crushing the EFBs to make them compatible with the fast pyrolysis process. Since the EFBs are small and have a low moisture content, the fast pyrolysis mechanism can be substantially improved to achieve the best bio-oil yield and quality. Following pretreatment, EFBs can be transferred for fast pyrolysis (A200), whereby they are decomposed to form a number of valuable products such as bio-oil, biochar, and syngas. These pyrolytic products are separated from each other in the separation system (A300). This is achieved by utilising cyclone equipment to remove the biochar, and flash drums to condensate the bio-oil out of incondensable vapour. The by-products are then used for heat recovery (A400) within the plant. This study assumes that the optimisation process only concerns the distillation section (A600).

The bio-oil produced during the fast pyrolysis process is introduced into the hydrotreatment process. This hydrotreatment requires pure H_2 gases to remove the unwanted compounds, as mentioned in the introduction section. The hydrotreatment process provides higher yields and improves the quality of pyrolysed bio-oil [15]. During

Journal of Energy Resources Technology. Received August 05, 2020;
Accepted manuscript posted April 05, 2021. doi:10.1115/1.4050817

Journal of Energy Resources Technology

this process, the temperature and pressure reach 387 °C and 87 bars, respectively. After the bio-oil has been hydrotreated, it is then fed into the separation process, comprising two distillation columns. The first distillation column is used to separate the gasoline from the heavy fraction. The role of the second (diesel) column is to allow the biodiesel to be separated out of the heavy compounds. Once distillation is complete, the hydrocracking process begins to treat the remaining heavy compounds. The hydrocracking process also utilises H_2 gas to extract some of the precious material inside the heavy compounds for recycling to the distillation process. A schematic of the upgrading section is shown in Fig. 2. The main operating conditions of the upgrading section are detailed in Table 1.

As previously mentioned, the diesel generator is developed in MATLAB. The theoretical equation is used to determine the energy output of the diesel generator according to the specific amount of biodiesel introduced.

The simple diagram in Fig. 3 represents the working cycle of an internal combustion diesel engine. At point 1, the cylinder locates at the bottom dead centre (BDC), the inlet and exhaust valves have just recently closed, with the atmospheric air already filling the entire combustion chamber. At point 2, the cylinder moves upwards from BDC to top dead centre (TDC) to compress all the air to create high pressure, generally raising the temperature inside the combustion chamber. In point 3, since the air has been completely pressurised, the fuel injection operates to feed the fuel into the chamber. Once the air and fuel have become completely mixed at point 3 inside the combustion chamber, the mixture ignites, rapidly expanding the chamber under a process of

Journal of Energy Resources Technology. Received August 05, 2020;
Accepted manuscript posted April 05, 2021. doi:10.1115/1.4050817

Journal of Energy Resources Technology

constant pressure. At point 4, the pressure of the burnt substances is reduced due to the general expansion of the combustion chamber as a result of the cylinder moving downwards to BDC. At point 5, the combustion process is complete, with the pressure and temperature of flue gas being relatively low due to the burning mechanism. Points 6 and 7 represent the exhaust process. The exhaust valve is open and the flue gas flows out of the combustion chamber aided by the cylinder moving upwards to TDC. The piston then moves down to BDC, with the inlet valve simultaneously opening to draw air from the atmosphere into the combustion chamber. This takes the combustion system back to point 1, from where it began, to carry out the diesel engine cycle once again.

Some of the equations are as follows [16]:

$m_{as} = \eta_v \left[\frac{P_1 V_{cyl}}{R_a T_1} \right]$	1)	$Q_3^4 = (1 - k_{cv}) Q_R$	13)
$P_2 = P_1 \left[\frac{V_{cyl}}{V_{cv}} \right]^{\gamma}$	2)	$T_4 = \frac{Q_3^4}{m_{as} C_P} + T_3$	14)
$T_2 = \frac{P_2 V_{cv}}{m_{as} R_a}$	3)	$V_4 = \frac{m_{as} R_a T_4}{(P_4 = P_3)}$	15)
$W_1^2 = \frac{P_2 V_{cv} - P_1 V_{cyl.}}{1 - \gamma}$	4)	$W_3^4 = P_3 (V_4 - V_{cv})$	16)
$m_f = \frac{Q_f \times S.G. \times 2(rev/cycle)}{60 \times rpm}$	5)	$W_3^4 = P_3 (V_4 - V_{cv})$	17)
$AFR = \frac{m_{as}}{m_f}$	6)	$P_5 = P_4 \left[\frac{V_4}{V_5 = V_{cyl}} \right]^{\gamma}$	18)
$\lambda = \frac{AFR}{AFR_{sto}}$	7)	$T_5 = \frac{P_5 V_{cyl}}{m_{as} R_a}$	19)

Journal of Energy Resources Technology. Received August 05, 2020;
Accepted manuscript posted April 05, 2021. doi:10.1115/1.4050817

Journal of Energy Resources Technology

$\eta_c = 0.35332 + 0.56797\lambda - 0.12472\lambda^2$	8)	$W^5{}_4 = \frac{P_5 V_{cvl} - P_4 V_4}{1-\gamma}$	20)
$Q_R = \eta_c \times C_{fl} \times m_f$	9)	$Q_5{}^6 = m_{as} C_v (T_6 - T_5)$	21)
$Q^3{}_2 = k_{cv} \times Q_R$	10)	$W_6{}^7 = P_{atm}(V_{cv} - V_{cvl})$	22)
$T_3 = \frac{Q_2{}^3}{m_{as} C_v} + T_2$	11)	$W_l = W_7{}^1 + W_1{}^2 + W_3{}^4 + W_4{}^5 + W_6{}^7$	23)
$P_3 = \frac{m_{as} R_a T_3}{V_{cv}}$	12)		

Where η_v = Volumetric efficiency of engine, P_1 = Pressure of atmospheric air (kPa), V_{cyl} = Volume of internal combustion cylinder (m^3), R_a = Ideal gas constant (8.31 J K^{-1} mol^{-1}), T_1 = Temperature of atmospheric air (°C), V_{sv} = Stroke volume (m^3), V_{cv} = Clearance volume (m^3), γ = Isentropic expansion factor, m_f = required mass of fuel (kg), Q_f = rate of fuel consumption (L/hr), C_f = heating value of fuel (MJ/kg), k_{cv} = combustion performance at specific constant volume, C_v = Specific heat capacity at constant volume (J/(kg·K)), C_p = Specific heat capacity at constant pressure (J/(kg·K))

According to the above theoretical equations, many specifications relate to the geometry and properties of the diesel generator. In this case, some diesel generator specifications are used to calculate the equations. The specification details are provided by selecting a diesel generator that is available in Thailand, as shown in Table 2 and Table 3.

Journal of Energy Resources Technology. Received August 05, 2020;
Accepted manuscript posted April 05, 2021. doi:10.1115/1.4050817

Journal of Energy Resources Technology

2.2 Design of experiments

In the initial designated operating condition, the parameters might not provide the best conditions for achieving the defined objective. Hence, optimisation aims to accomplish the best design, according to a set of specific conditions or constraints. These include maximising factors such as the rate of production, benefit point, reliability, efficiency, and utilisation [17]. The objectives of this study should be assessed accordingly. The power plant under study should maximise its profitability to achieve financial satisfaction. The objectives of optimising gasoline yield and increasing the magnitude of electricity generation should then be achieved as a consequence of higher biodiesel yield. To achieve profit maximisation at the plant, it is important to take utility costs into account. Since the operation of the plant involves renewable technology, it is also necessary to consider carbon dioxide emissions. Therefore, this study has four objectives: (1) electricity generation (kW), (2) mass yield of gasoline, (3) utility cost, and (4) CO_2 emissions.

In terms of the dependent variable or varying factors, it is important to perform sensitivity analysis on these factors according to the objectives. In the existing literature, it is often argued that the main proportion of energy consumption in the type of plant under study will come from the distillation column, accounting for around half the total [18]. Therefore, the distillation column is an important aspect on which to focus. Many parameters potentially impact the ability of distillation in the column, such as operating pressure, reflux ratio, number of stages, product specifications, etc. [19]. To match the distillation column specification, the reflux ratio is selected as one of the variables. The

Journal of Energy Resources Technology. Received August 05, 2020;
Accepted manuscript posted April 05, 2021. doi:10.1115/1.4050817

Journal of Energy Resources Technology

other two variables are the pressure of the flash drum (FLSH-HDT) and temperature of the heat exchanger (COOL-HDT). These two devices initially separate the light hydrocarbons (C1-C4) and H_2 gas from the hydrotreated stream. Light hydrocarbons have an extremely low boiling point with an average value lower than 5 °C [20]. These light hydrocarbons are more toxic than heavy hydrocarbons [21]. Apart from the independent factors, the other parameters are assumed to have a constant value.

After specifying the independent factors, the levels were entered into the Design-Expert 12.0.8 (trial), and the experimental design matrix given, as shown in Table 4. According to the methodology used, 14 runs were obtained, using a randomised subtype, Box-Behnken design, and a quadratic model.

2.3 Economic parameters

From the economic perspective, consideration should be given to the operating conditions and the setting of clear boundaries set. The only boundary requiring consideration in this study is the operating phase, with the capital cost excluded from the calculation. The economic assumptions are shown in Table 5.

3 Results and Discussion

3.1 Optimisation process

For the Box-Behnken design, a total of 14 experimental runs for formulation are proposed by the Design-Expert software, focusing on three factors: the reflux ratio of gasoline column (A), temperature of the heat exchanger [COOL-HDT] (B), and pressure

Journal of Energy Resources Technology. Received August 05, 2020;
Accepted manuscript posted April 05, 2021. doi:10.1115/1.4050817

of the flash drums [FLSH-HDT] (C). These factors could be varied at three levels. The various effects of the independent factors on the generation of electricity are then examined, based on the properties of biodiesel (kW), plant utility costs (USD/hr), gasoline mass yield (kg/hr), and level of carbon dioxide emissions, for parameter optimisation. The expected values for the planned experiment, along with the recorded responses, are presented in Table 6.

According to Table 6, it can be observed that the set of independent factors are the same for both experiments 6 and 14. It is possible to ignore these particular experiment sets to achieve a more concise optimisation process. The set of responses are used to develop the polynomial equation as a representative system model. The polynomial equations are presented as a relation between the independent factors and defined objectives of this study.

The developed equation is analysed as a representative model of the system. The results of the analysis are shown in Table 7. It can be observed that if the P-value of any factor is lower than the significance level of 0.05, the factor can be considered significant with a confidence level of 95%. The model of electricity generation, mass flow rate of gasoline, utility cost, and CO_2 emissions are revealed to be significant with predicted R-squared values of 0.9902, 0.9799, 0.9999, and 0.9999, respectively. The model proposes the following polynomial equations for electricity generation (Y_1), mass yield of gasoline (Y_2), utility cost (Y_3), and CO_2 emissions (Y_4), respectively:

$$Y_1 = 101.55556 + 0.63864A + 0.00412B + 0.31133C - 0.00582AB - 0.00255AC + \quad (24)$$

Journal of Energy Resources Technology. Received August 05, 2020;
Accepted manuscript posted April 05, 2021. doi:10.1115/1.4050817

Journal of Energy Resources Technology

$$0.00181BC - 0.12727A^2 - 0.00089B^2 - 0.0052C^2$$

214

$$Y_2 = 20.6308 - 0.0989A + 0.0402B - 0.2131C + 0.0003AB + 0.0023AC + 0.0023BC + 0.0101A^2 - 0.0005B^2 - 0.0015C^2 \quad (25)$$

215

$$Y_3 = 31.45617 + 0.18484A - 0.00986B + 0.01011C + 0.0032AB - 0.0006AC - 0.00001BC + 0.01487A^2 - 0.00002B^2 - 0.0001C^2 \quad (26)$$

216

$$Y_4 = 140.8185 + 0.82562A - 0.04436B + 0.04467C + 0.00144AB - 0.0027AC - 0.00006BC + 0.067778A^2 - 0.00007B^2 - 0.00043C^2 \quad (27)$$

217 A linear graph plot of the responses, as a result of varying the independent factors, is
218 shown in Fig. 4, denoting the comparison between predicted and simulation values of
219 electricity generation, the mass flow rate of gasoline, utility cost, and CO_2 emissions by
220 Y_1, Y_2, Y_3, Y_4, respectively. It can be observed that the developed linear correlation fits
221 well with the actual value.

222 Details of the suggested conditions for each independent factor contributing to the
223 optimum value of the specified criteria, along with the constraints, are presented in
224 Table 8. It can be observed that the predicted values are not significantly different from
225 the actual values. The percentage errors for electricity generation, yield of gasoline,
226 utility cost, and CO_2 emissions are 0.012, 0.028, 0.007, and 0.006%, respectively. A
227 three-dimensional response graph is appropriate for studying the related effects of the
228 independent factors on the designed responses, as shown in Fig. 5.

Journal of Energy Resources Technology. Received August 05, 2020;
Accepted manuscript posted April 05, 2021. doi:10.1115/1.4050817

Journal of Energy Resources Technology

229 The increase in pressure (15 to 25 bars) illustrates the rising electricity generation
230 (100.66 to 105.99 kW) resulting from the higher biodiesel yield (Fig. 5a). However, the
231 rising temperature (60 to 90 °C) gives the opposite result in that it decreases the
232 magnitude of electricity generation. This might be due to the higher vapourisation of
233 hydrocarbon compounds. The decrease in pressure (25 to 15 bars) in Fig. 5b causes an
234 increase in the mass yield of gasoline (18.39 to 19.78 kg/hr)—the rise in temperature
235 creating an increasing trend in gasoline yield. The highest possible value generated for
236 gasoline yield (19.78 kg/hr) can be achieved at a temperature of 75 °C and a pressure of
237 15 bars. The decrease in reflux ratio (1.25 to 0.15) in Fig. 5c favours lower utility costs
238 (31.23 to 30.60 USD/hr) due to correspondingly lower energy consumption [30]. In
239 terms of the temperature in the heat exchanger, when it is increased (60 to 90 °C), the
240 utility cost decreases. The heat exchanger is responsible for heating the bio-oil to
241 improve the separation process in the flash drum. When it reaches the optimum
242 temperature, greater extraction of lighter hydrocarbon can be achieved. Consequently,
243 higher temperatures, lower the feeding rate of the distillation column, thereby reducing
244 the effort required by the equipment. The relationship between CO_2 emissions,
245 temperature, and pressure is examined, as shown in Fig. 5d. This gives a similar result to
246 the response surface of the utility cost. An increase in temperature (60 to 90 °C) raises
247 the CO_2 emissions, while a decrease in pressure lowers the CO_2 emissions.
248
249
250

Journal of Energy Resources Technology. Received August 05, 2020;
Accepted manuscript posted April 05, 2021. doi:10.1115/1.4050817

3.2 Economic analysis

Besides the optimum solution (scenario 1 in Table 9) suggested by the software, other alternative solutions can be considered for economic analysis, as shown in Table 10. These scenarios offer various advantages such as increased production capacity, economic profitability, and reduced CO_2 emissions.

Table 8 shows that three different situations can provide varying responses. In scenario 2, the utility cost (30.615 USD/hr) and carbon dioxide emissions (137.04 kg/hr) are both at the lowest levels among all sets of responses. Scenario 3 provides the highest electricity generation of 103.38 kW among all sets of responses, while scenario 4 provides the highest gasoline production yield (19.78 kg/hr) but the lowest value for electricity generation (102.71 kW). These three response sets will be used for further analysis from the economic perspective. The economic assumptions and method of calculation have already been provided in Table 4.

The responses of these scenarios can be used to calculate the utility cost, electricity sale price, gasoline sale price, and the magnitude of CO_2 emissions. Details of both the base case, which is the original plant without the benefit of optimisation, and the scenarios, with the advantage of optimisation, are presented in Table 9.

The results of economic analysis and CO_2 emissions are shown in Fig. 6. It is clear that in scenario 4, where the highest level of gasoline production and maximum profitability of 7,481 USD/yr can be achieved, carbon dioxide emissions are also the highest recorded at 827 tons/yr. In scenario 2, these independent variable sets can offer the best performance for an environmentally-friendly power plant, producing just 822

Journal of Energy Resources Technology. Received August 05, 2020;
Accepted manuscript posted April 05, 2021. doi:10.1115/1.4050817

Journal of Energy Resources Technology

tons of CO_2/yr in emissions. However, in economic terms, it contributed the smallest profit of all scenarios. To fulfil both economic and environmental requirements, the scenario suggested by the Design-Expert might be the optimum response (scenario 1), since the profit is almost the highest at 5,571 USD/yr, with the CO_2 emissions almost the lowest at 824 tons CO_2/yr, among all scenarios. However, the choice of suitable factors for successful operation will be dependent upon the power plant objectives. If the project owner considers profitability to be a priority, scenario 4 might be the most suitable option. However, if the owner wishes to focus on the environmental issue, scenario 2 is the best option for sustainable technology utilisation. In order to propose the designed model, a modern technology called deep learning [31,32] can be implemented. This will help investors to make decision while introducing into a smart grid.

4 Conclusion

This study examines the use of EFBs for generating electrical power. The efficient production of electricity requires EFBs to firstly undergo conversion into biofuel. The power plant then uses a fast pyrolysis process for the conversion. However, in optimising the operation of the power plant, the environmental impact and economic outcomes cannot be ignored. For this reason, RSM is employed in the optimisation process. The simulation findings reveal that in the initial base condition with no optimisation, the following results were achieved for power generation (105.81 kW), gasoline mass yield (18.78 kg/hr), utility cost (31.34 USD/hr), and carbon dioxide

Journal of Energy Resources Technology. Received August 05, 2020;
Accepted manuscript posted April 05, 2021. doi:10.1115/1.4050817

295 emissions (140.28 kg/hr). The optimisation using Design-Expert V.12.0.8 (trial) software,
296 proposed the optimum point for the reflux ratio of GASOCOL at 0.15, while the
297 temperature of COOL-HDT should be 85.17 °C, with the FLSH-HDT pressure at 21.07 bar.
298 With the independent factors optimised, the following results were reported for power
299 generation (102.99 kW), gasoline mass yield (19.27 kg/hr), utility cost (30.67 USD/hr),
300 and carbon dioxide emissions (137.29 kg/hr). The outcome in terms of profit was an
301 annual increase of 3,836 USD, while carbon dioxide emissions declined by 17.97 tons
302 annually. Although this scenario is optimised from the economic and environmental
303 perspective, an alternative exists which would maximise profitability but, unfortunately,
304 also yield the highest carbon dioxide emissions. Meanwhile, another choice offers
305 superior environmental performance but minimises profit. In this case, the decision
306 must fall to the owner of the plant, who must decide which scenario to favour,
307 according to the objectives of the business. In any event, the optimised approach will be
308 superior to the non-optimised alternatives.

309 This work's limitation is that the biodiesel power plant model developed on Aspen
310 Plus software might not be entirely and perfectly validated because of the lack of an
311 actual prototype of the plant utilised to reference results. Recently, the problem of EFB
312 in terms of the environment has been widely concerned. Many institutions try many
313 different ways to utilise the EFB as material for the commercialised product properly.
314 Fast pyrolysis is one of the promising technologies. The full cycle of operation utilised
315 the fast pyrolysis, as a core bioconversion process, has not completely developed. The
316 future of the present work might be further analysis on the uncertainty of the individual

Journal of Energy Resources Technology. Received August 05, 2020;
Accepted manuscript posted April 05, 2021. doi:10.1115/1.4050817

process. The improvement in economic assessment might be required to achieve more on the accuracy of profitability evaluation.

ACKNOWLEDGEMENT

This work was supported the computer device and working place by Rajamangala University of Technology (RMUTT) Thailand. This research is supported by the Thailand Advanced Institute of Science and Technology and Tokyo Institute of Technology (TAIST-Tokyo Tech) program under the National Science and Technology Development Agency (NSTDA). This research was also supported by grants funded by the National Research Council of Thailand (NRCT) and the Research University Network.

FUNDING

The authors declare that they have no known competing financial interests or personal relationships that could appear to influence the work reported in this paper.

REFERENCES

[1] Sutabutr, T., *Alternative energy development plan: AEDP 2012-2021.* Journal of Renewable Energy and Smart Grid Technology, 2012. **7**(1): p. 1-10.

[2] Chanlongphitak, S., Papong, S., Malakul, P. and Mungcharoen, T., 2015, "Life cycle assessment of palm empty fruit bunch utilization for power plants in Thailand," In *International Conference on Biological, Environment and Food Engineering: Singapore. http://iicbe. org/upload/4352 C* (Vol. 515048).

Journal of Energy Resources Technology. Received August 05, 2020;
Accepted manuscript posted April 05, 2021. doi:10.1115/1.4050817

[3] Choojit, S. and Sangwichien, C., 2018, "PREPARATION OF ACTIVATED CARBON PRODUCTION FROM OIL PALM EMPTY FRUIT BUNCH AND ITS APPLICATION," *Kasem Bundit Engineering Journal*, ***8***(2), pp.48-67.

[4] Mansora, A.M., Lima, J.S., Anib, F.N., Hashima, H. and Hoa, W.S., 2019, "Characteristics of cellulose, hemicellulose, and lignin of MD2 pineapple biomass," CHEMICAL ENGINEERING, 72.

[5] Barz, M. and Delivand, M.K., 2011, "Agricultural residues as promising biofuels for biomass power generation in Thailand," *Journal of Sustainable Energy & Environment Special Issue*, *21*, p.27.

[6] Riva, G., Pedretti, E.F., Toscano, G., Duca, D. and Pizzi, A., 2011, "Determination of polycyclic aromatic hydrocarbons in domestic pellet stove emissions," *Biomass and bioenergy*, ***35***(10), pp.4261-4267.

[7] Lim, M.T., Phan, A., Roddy, D. and Harvey, A., 2015, "Technologies for measurement and mitigation of particulate emissions from domestic combustion of biomass: A review," *Renewable and Sustainable Energy Reviews*, *49*, pp.574-584.

[8] Pattiya, A., Titiloye, J.O., and Bridgwater, A.V., 2009, 'Fast pyrolysis of agricultural residues from cassava plantation for bio-oil production," *Carbon*, *51*, pp.51-59.

[9] Xu, Y., Hu, X., Li, W. and Shi, Y., 2011, "*Preparation and characterization of bio-oil from biomass,*" (pp. 197-222). InTech Publisher: Rijeka, Croatia.

[10] Zheng, J.L. and Wei, Q., 2011, "Improving the quality of fast pyrolysis bio-oil by reduced pressure distillation," *Biomass and Bioenergy*, ***35***(5), pp.1804-1810.

[11] Araujo, P.W. and Brereton, R.G., 1996, "Experimental design I. Screening," *TrAC Trends in Analytical Chemistry*, ***15***(1), pp.26-31.

[12] Asghar, A., Abdul Raman, A.A. and Daud, W.M.A.W., 2014, "A comparison of central composite design and Taguchi method for optimizing Fenton process," *The Scientific World Journal*, *2014*.

[13] Bezerra, M.A., Santelli, R.E., Oliveira, E.P., Villar, L.S. and Escaleira, L.A., 2008, "Response surface methodology (RSM) as a tool for optimization in analytical chemistry," *Talanta*, ***76***(5), pp.965-977.

[14] Kerdsuwan, S. and Laohalidanond, K., 2011, "Renewable energy from palm oil empty fruit bunch" *Renewable energy-trends and applications*, pp.123-150.

Journal of Energy Resources Technology. Received August 05, 2020;
Accepted manuscript posted April 05, 2021. doi:10.1115/1.4050817

[15] Auersvald, M., Shumeiko, B., Vrtiška, D., Straka, P., Staš, M., Šimáček, P., Blažek, J. and Kubička, D., 2019, "Hydrotreatment of straw bio-oil from ablative fast pyrolysis to produce suitable refinery intermediates," *Fuel*, *238*, pp.98-110.

[16] Vathakit, K., 2012, "A Study of Boost Pressure on Efficiency of an Agricultural Single Cylinder Diesel Engine – Theory and Calculations," in *TSAE International Conference*, Chiang Mai: TSAE – Thai Society of Agricultural Engineering.

[17] Merrill, C., Custer, R.L., Daugherty, J.L., Westrick, M. and Zeng, Y., 2008, "Delivering core engineering concepts to secondary level students," *Volume 20 Issue 1 (fall 2008)*.

[18] Lee, J., Son, Y., Lee, K.S. and Won, W., 2019, "Economic analysis and environmental impact assessment of heat pump-assisted distillation in a gas fractionation unit," *Energies*, ***12***(5), p.852.

[19] Cui, C., Liu, S. and Sun, J., 2018, "Optimal selection of operating pressure for distillation columns," *Chemical Engineering Research and Design*, ***137***, pp.291-307.

[20] Group, T.P.H.T., 2009, "PETROLEUM HYDROCARBON GASES CATEGORY ANALYSIS AND HAZARD CHARACTERIZATION," HPV Consortium Registration. p. 145.

[21] Labud, V., Garcia, C. and Hernandez, T., 2007, "Effect of hydrocarbon pollution on the microbial properties of a sandy and a clay soil," *Chemosphere*, ***66***(10), pp.1863-1871.

[22] Delivand, M.K., Barz, M. and Gheewala, S.H., 2011, "Logistics cost analysis of rice straw for biomass power generation in Thailand," *Energy*, ***36***(3), pp.1435-1441.

[23] (EforE), E.f.E.F., *Project of studying and analysis of utilization of renewable energy report in local private enterprise and small industrial of Thailand*. 2017: Energy for Environment Foundation (EforE). p. 20.

[24] (MEA), M.E.A. *Medium General Service of electricity (Applicability)*,2018, *Accessed on 27 April 2020*; Available from: https://www.mea.or.th/download/view/26327.

[25] Promjiraprawat, K. and Limmeechokchai, B., 2013, "Multi-objective and multi-criteria optimization for power generation expansion planning with CO_2 mitigation in Thailand," *Songklanakarin Journal of Science & Technology*, ***35***(3).

[26] Delivand, M.K., Barz, M., Gheewala, S.H. and Sajjakulnukit, B., 2011, "Economic feasibility assessment of rice straw utilization for electricity generating through combustion in Thailand," *Applied Energy*, ***88***(11), pp.3651-3658.

[27] Labour, M.o. *Minimum wage*. [Website] 1 January 2020 [cited 9 April 2020]; Available from: https://www.mol.go.th/en/minimum-wage/.

Journal of Energy Resources Technology. Received August 05, 2020;
Accepted manuscript posted April 05, 2021. doi:10.1115/1.4050817

[28] www.GlobalPetrolPrices.com. *Thailand Gasoline prices, Accessed on: 30-Mar-2020.* 2020; Available from: https://www.globalpetrolprices.com/Thailand/gasoline_prices/.

[29] Tantisattayakul, T. and Kanchanapiya, P., 2017, "Financial measures for promoting residential rooftop photovoltaics under a feed-in tariff framework in Thailand," *Energy policy*, ***109***, pp.260-269.

[30] De Figueiredo, M.F., Brito, K.D., Ramos, W.B., Sales Vasconcelos, L.G. and Brito, R.P., 2015, "Effect of solvent content on the separation and the energy consumption of extractive distillation columns," *Chemical Engineering Communications*, ***202***(9), pp.1191-1199.

[31] Prabadevi, B., Quoc-Viet, P., Madhusanka, L., Deepa, N., Mounik, VVSS., and Shivani, R., 2021, "Deep Learning for Intelligent Demand Response and Smart Grids: A Comprehensive Survey," Computer Science, arXiv:2101.08013

[32] Alazab, M., (Senior Member, IEEE), Khan, S., Krishnan, S.S.R., Pham, Q.V., (Member, IEEE), Praveen Kumar Reddy, M., and Thippa Reddy, G., 2020, "A Multidirectional LSTM Model for Predicting the Stability of a Smart Grid," IEEE Access, **8**, pp. 85454 - 85463.

Journal of Energy Resources Technology. Received August 05, 2020;
Accepted manuscript posted April 05, 2021. doi:10.1115/1.4050817

476
477
478

Figure Captions List

Fig. 1 Pretreatment section (A100), Pyrolysis section (A200), Separation section (A300), Combustion section (A400)

Fig. 2 Hydrotreating section (A500), Distillation section (A600), Hydrocracking section (A700)

Fig. 3 Theoretical PV diagram of diesel cycle

Fig. 4 Linear correlation plot between the simulation and predicted response

Fig. 5 a) Effect of temperature of COOL-HDT & pressure of FLSH-HDT on electricity generation. (b) Effect of temperature of COOL-HDT & pressure of FLSH-HDT on the mass yield of gasoline. (c) Effect of temperature of COOL-HDT & reflux ratio of GASOCOL on utility cost. (d) Effect of temperature of COOL-HDT & pressure of FLSH-HDT on CO_2 emission

479 Fig. 6 Profitability and CO_2 emission of each scenarios

480
481
482
483
484
485
486
487
488
489
490
491
492
493
494
495
496
497

Journal of Energy Resources Technology. Received August 05, 2020;
Accepted manuscript posted April 05, 2021. doi:10.1115/1.4050817

Journal of Energy Resources Technology

498 **Table Caption List**
499

500
501
502
503
504
505
506
507
508
509
510
511
512
513

Journal of Energy Resources Technology. Received August 05, 2020;
Accepted manuscript posted April 05, 2021. doi:10.1115/1.4050817

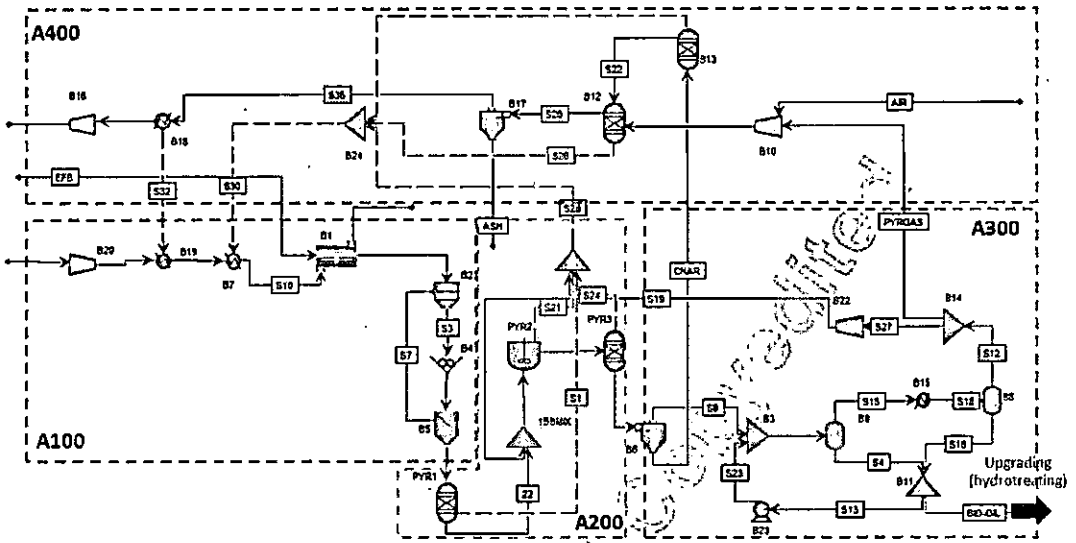

Fig. 1 Pretreatment section (A100), Pyrolysis section (A200), Separation section (A300), Combustion section (A400)

Journal of Energy Resources Technology. Received August 05, 2020;
Accepted manuscript posted April 05, 2021. doi:10.1115/1.4050817

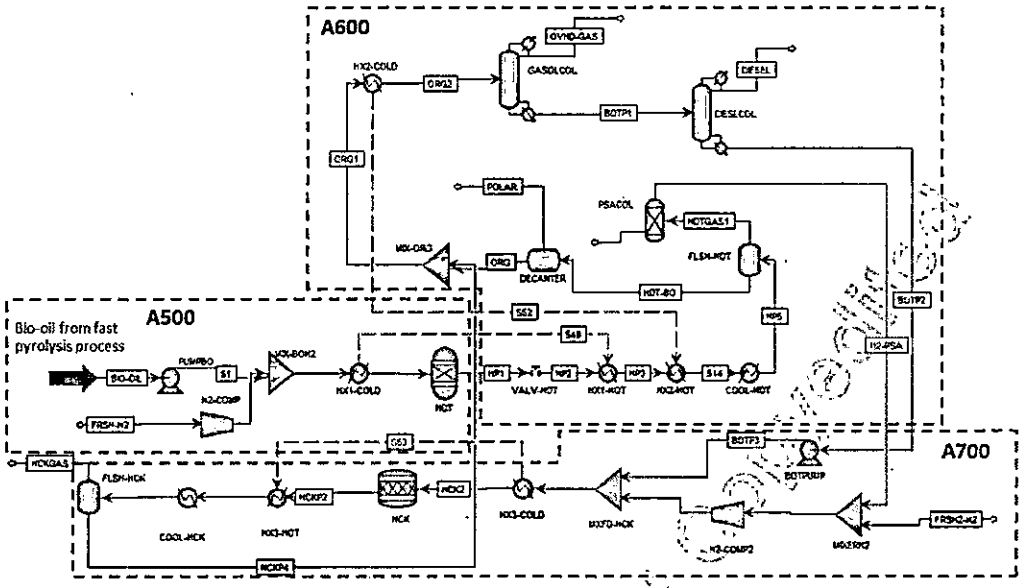

Fig. 2 Hydrotreating section (A500), Distillation section (A600), Hydrocracking section (A700)

Journal of Energy Resources Technology. Received August 05, 2020;
Accepted manuscript posted April 05, 2021. doi:10.1115/1.4050817

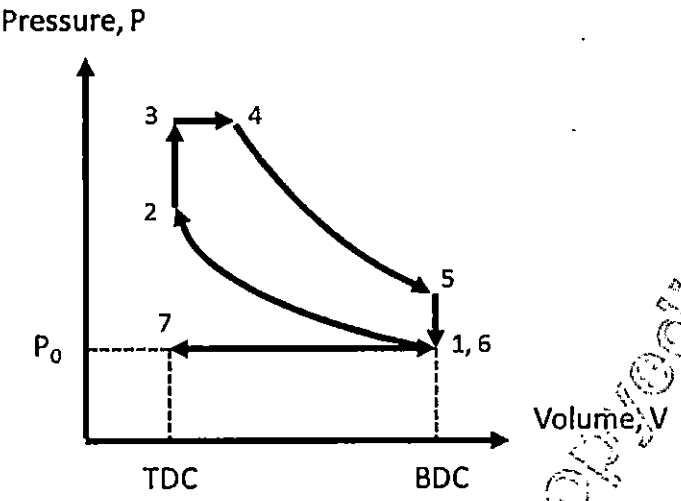

Fig. 3 Theoretical PV diagram of diesel cycle

Journal of Energy Resources Technology. Received August 05, 2020;
Accepted manuscript posted April 05, 2021. doi:10.1115/1.4050817

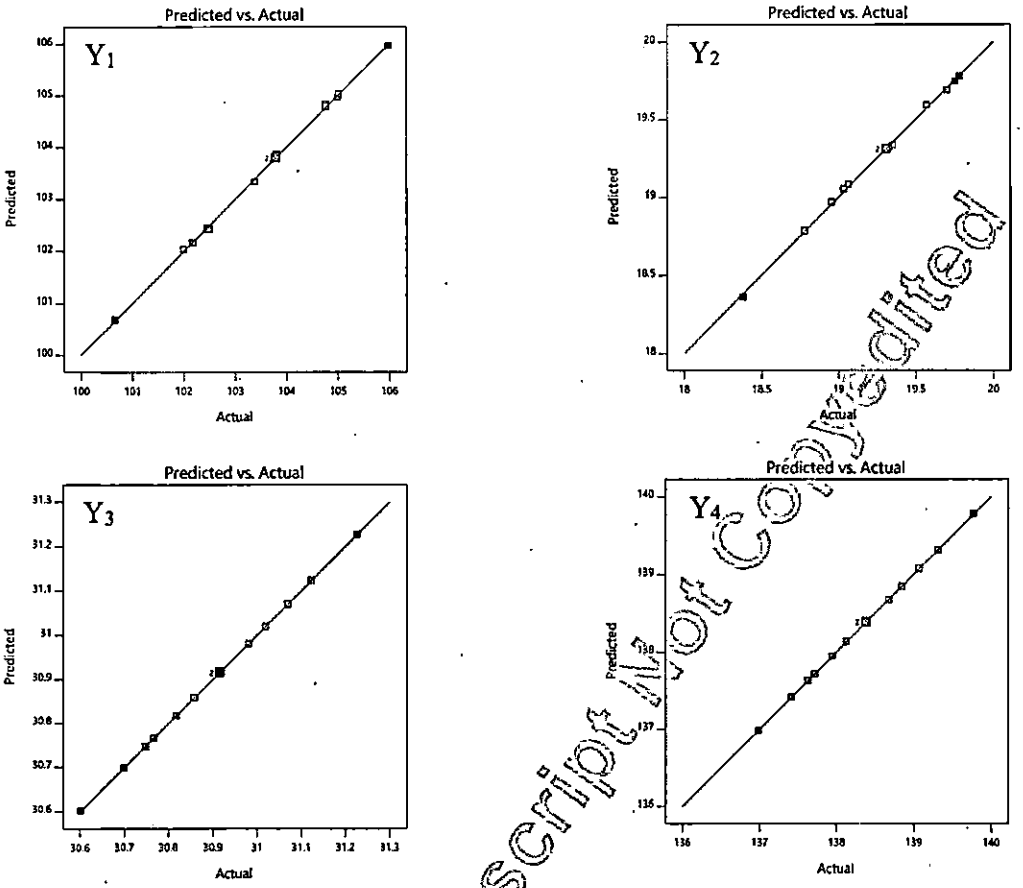

Fig. 4 Linear correlation plot between the simulation and predicted response

Journal of Energy Resources Technology. Received August 05, 2020;
Accepted manuscript posted April 05, 2021. doi:10.1115/1.4050817

Journal of Energy Resources Technology

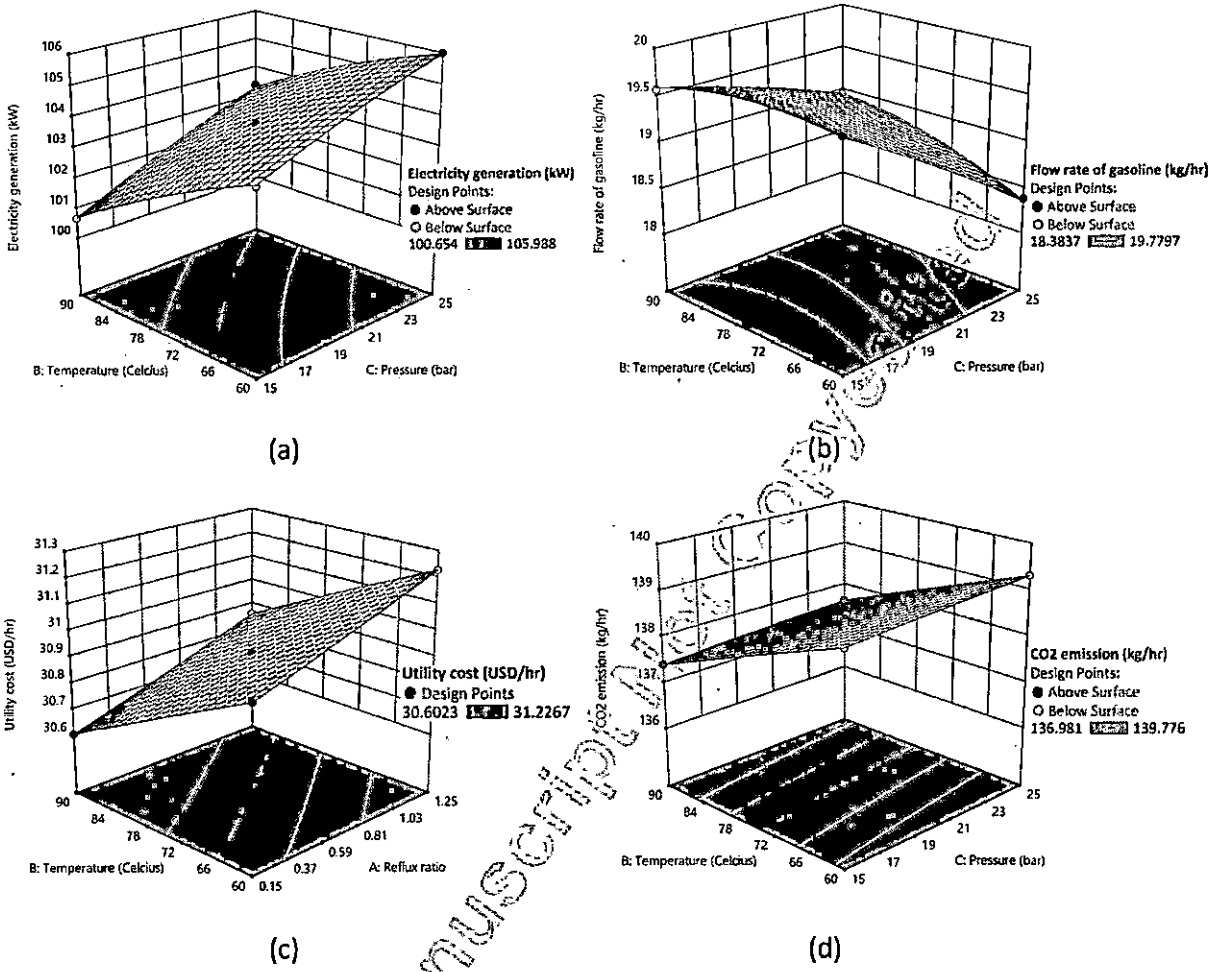

Fig. 5 (a) Effect of temperature of COOL-HDT & pressure of FLSH-HDT on electricity generation. (b) Effect of temperature of COOL-HDT & pressure of FLSH-HDT on the mass yield of gasoline. (c) Effect of temperature of COOL-HDT & reflux ratio of GASOCOL on utility cost. (d) Effect of temperature of COOL-HDT & pressure of FLSH-HDT on CO_2 emission

Journal of Energy Resources Technology. Received August 05, 2020;
Accepted manuscript posted April 05, 2021. doi:10.1115/1.4050817

644

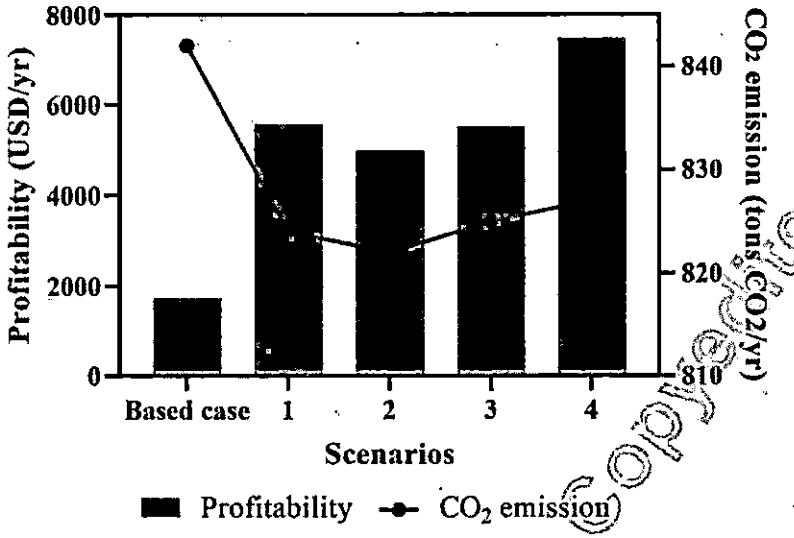

645

646 **Fig. 6 Profitability and CO_2 emission of each scenarios**

647
648
649
650
651
652
653
654
655
656
657
658
659
660
661
662
663
664
665
666
667
668
669
670
671
672
673

Journal of Energy Resources Technology. Received August 05, 2020;
Accepted manuscript posted April 05, 2021. doi:10.1115/1.4050817

Journal of Energy Resources Technology

674 **Table 1 Composition of EFB [14]**
675

Elemental composition	Air-dried basis (% wt.)
Carbon	43.80
Hydrogen	6.20
Oxygen	42.64
Nitrogen	0.44
Sulfur	0.09
Others	0.53
Ash	6.30
Proximate composition	
Moisture	8.34
Volatile	73.16
Ash	6.30
Fixed Carbon	12.20

676
677
678
679
680
681
682
683
684
685
686
687
688
689
690
691
692
693
694
695
696
697
698
699
700
701
702
703
704
705

Journal of Energy Resources Technology. Received August 05, 2020;
Accepted manuscript posted April 05, 2021. doi:10.1115/1.4050817

Journal of Energy Resources Technology

706 **Table 2 Important operating condition of key equipment**
707

Sections	Key equipment	Operating conditions
Hydrotreating (A500)	Hydrotreating reactor (HDT)	Temperature: 387 °C Pressure: 87 bar
Distillation (A600)	Heat exchanger (COOL-HDT)	Temperature: 50 °C Pressure: 20 bar
	Flash drum (FLSH-HDT)	Pressure: 20 bar
	Gasoline column (GASOLCOL)	Mass reflux ratio: 1.2 *Mass-to-distillate ratio: 0.440 Number of stages: 9
	Diesel column (DIESLCOL)	Mass reflux ratio: 1.2 *Mass-to-distillate ratio: 0.897 Number of stages: 8
Hydrocracking (A700)	Hydrocracking reactor (HCK)	Temp: 670 °C Pressure: 90 bar

708 * Mass-to-distillate ratio obtained from the using of 'design spec' tool in Aspen Plus
709 software. This ratio should be specified to achieve the typical distillate gasoline and
710 biodiesel specification.
711
712
713
714
715
716
717
718
719
720
721
722
723
724
725
726
727
728
729
730
731
732
733
734
735

Journal of Energy Resources Technology. Received August 05, 2020;
Accepted manuscript posted April 05, 2021. doi:10.1115/1.4050817

Journal of Energy Resources Technology

736 **Table 3 Important specification of diesel generator**
737

Specifications	Units	Values
Engine speed	RPM	1,800
Total displacement	Liter	5.9
Bore x Stroke	mm x mm	102 x 120
Max. fuel consumption	Liter/hr	30.7
Number of cylinders	-	6-inline
Compression ratio	-	17.3:1

738
739
740
741
742
743
744
745
746
747
748
749
750
751
752
753
754
755
756
757
758
759
760
761
762
763
764
765
766
767
768
769
770
771
772

Journal of Energy Resources Technology. Received August 05, 2020;
Accepted manuscript posted April 05, 2021. doi:10.1115/1.4050817

773 **Table 4 The design matrix of the experiment**
774

Run	Reflux ratio of GASOCOL	Temperature of COOL-HDT (°C)	Pressure of FLSH-HDT (bar)
1	0.70	60	25
2	0.70	90	15
3	1.25	90	20
4	0.15	90	20
5	0.70	60	15
6	0.70	75	20
7	1.25	60	20
8	1.25	75	15
9	0.70	90	25
10	0.15	60	20
11	0.15	75	15
12	0.15	75	25
13	1.25	75	25
14	0.70	75	20

775
776
777
778
779
780
781
782
783
784
785
786
787
788
789
790
791
792
793
794
795
796
797
798
799
800

Journal of Energy Resources Technology. Received August 05, 2020;
Accepted manuscript posted April 05, 2021. doi:10.1115/1.4050817

Table 5 Economic assumptions

Economic items	Value	Ref.
* Operation duration (hr/year)	6,000	[22]
Price of EFB (USD/ton)	15.30	[23]
Electricity cost (USD/unit)	0.11	[24]
Operation and Maintenance cost (O&M)		[25]
Fixed O&M (USD/yr)	3,480	
Variable O&M (USD/MWh)	0.97	
Labor cost		
Number of workers (person)	$13.791\ (MWe)^{0.4328}$	[26]
Wage of worker (USD/person/day)	10.5	[27]
Gasoline selling price (USD/L)	0.74	[28]
* Electricity income (USD/unit)	0.185	[29]

* This was made as to the assumption of the estimated total operating hour per year
** This electricity income is calculated based on the consideration as this power plant is a renewable technology, Feed-in Tariffs. Thai government provides a special price for any power generation that coming from renewable sources.

Journal of Energy Resources Technology. Received August 05, 2020;
Accepted manuscript posted April 05, 2021. doi:10.1115/1.4050817

Journal of Energy Resources Technology

Table 6 Experimental matrix of Box-Behnken design with defined response values

Run No.	Level of factors employed			Responses			
	A (-)	B (°C)	C (bar)	Y_1 (kW)	Y_2 (kg/hr)	Y_3 (USD/hr)	Y_4 (kg/hr)
1	0.70	60	25	105.99	18.38	31.123	139.31
2	0.70	90	15	100.65	19.57	30.700	137.42
3	1.25	90	20	102.00	19.33	30.858	138.13
4	0.15	90	20	102.18	19.35	30.602	136.98
5	0.70	60	15	103.81	19.70	31.070	139.08
6	0.70	75	20	103.78	19.31	30.916	138.39
7	1.25	60	20	105.02	19.03	31.227	139.78
8	1.25	75	15	102.49	19.75	31.020	138.85
9	0.70	90	25	103.38	18.96	30.748	137.63
10	0.15	60	20	104.99	19.06	30.981	138.68
11	0.15	75	15	102.45	19.78	30.767	137.72
12	0.15	75	25	104.77	18.78	30.818	137.95
13	1.25	75	25	104.77	18.78	31.070	139.07
14	0.70	75	20	103.79	19.31	30.917	138.39

Where A = Reflux ratio of GASOCOL, B = Temperature of COOL-HDT (°C), C = Pressure of FLSH-HDT (bar), Y_1 = Electricity generation (kW), Y_2 = Mass flow rate of gasoline (kg/hr), Y_3 = Utility cost (USD/hr), Y_4 = CO_2 emission (kg/hr)

Journal of Energy Resources Technology. Received August 05, 2020;
Accepted manuscript posted April 05, 2021. doi:10.1115/1.4050817

Table 7 ANOVA of linear, quadratic and interactive terms of the biodiesel power plant on responses (P-value)

Items	Electricity generation (kW)	Mass flow rate of gasoline (kg/hr)	Utility cost (USD/hr)	CO_2 emission (kg/hr)
Model	< 0.001*	< 0.001*	< 0.001*	< 0.001*
A-reflux ratio of distillation column	0.560	0.334	< 0.001*	< 0.001*
B-temp. of heat exchanger	< 0.001*	0.001*	< 0.001*	< 0.001*
C-pressure flash drum	< 0.001*	< 0.001*	< 0.001*	< 0.001*
A*B	0.218	0.875	0.001*	0.001*
A*C	0.842	0.655	0.653	0.648
B*C	0.014*	< 0.001*	0.034*	0.033*
A*A	0.354	0.845	< 0.001*	< 0.001*
B*B	0.006*	< 0.001*	< 0.001*	< 0.001*
C*C	0.024*	0.058	0.003*	0.003*
R^2	0.994	0.999	1.000	1.000

* significant

Journal of Energy Resources Technology. Received August 05, 2020;
Accepted manuscript posted April 05, 2021. doi:10.1115/1.4050817

Journal of Energy Resources Technology

885 **Table 8 Comparison of predicted value as a result of optimizations with actual**
886 **response values from the simulation**
887

Constraints (Independent factors)	Target (importance)	Experimental range	Optimal value	
Independent factors				
Reflux ratio	In range	0.15 – 1.25	0.15	
The temperature of COOL-HDT (°C)	In range	60 – 90	85.17	
Pressure of FLSH-HDT (bars)	In range	15 – 25	21.07	
Responses			**Predicted value**	**Actual value**
Electricity generation (kW)	Maximize	100.65 - 105.99	102.99	102.98
Mass yield of gasoline (kg/hr)	Maximize	18.38 - 19.78	19.27	19.27
Utility cost (USD/hr)	Minimize	30.602 - 31.227	30.673	30.672
CO_2 emission (kg/hr)	Minimize	136.98 - 139.78	137.29	137.28

888
889
890
891
892
893
894
895
896
897
898
899
900
901
902
903
904
905
906
907
908
909
910
911
912

Journal of Energy Resources Technology. Received August 05, 2020;
Accepted manuscript posted April 05, 2021. doi:10.1115/1.4050817

913 **Table 9 The alternative scenarios of the responses**

914

Scenarios	Reflux ratio of distillation column	Temp. of heat exchanger (°C)	Pressure of flash drum (bar)	Electricity generation (kW)	Yield of gasoline (kg/hr)	Utility cost (USD/yr)	CO_2 emission (kg/hr)
1 (optimum value)	0.15	85.17	21.07	102.99	19.27	30.67	137.29
2	0.15	90.00	22.75	102.85	19.14	30.62	137.04
3	0.15	82.64	21.58	103.38	19.22	30.71	137.44
4	0.15	72.51	15.07	102.71	19.78	30.80	137.86

915
916
917
918
919
920
921
922
923
924
925
926
927
928
929
930
931
932
933
934
935
936
937
938
939
940
941
942
943
944
945
946

Journal of Energy Resources Technology. Received August 05, 2020;
Accepted manuscript posted April 05, 2021. doi:10.1115/1.4050817

Journal of Energy Resources Technology

947 **Table 10 Economic comparison between the scenarios and the base case**
948

	Scenarios				
	Base case	1 (optimum condition)	2	3	4
Cost (USD/yr)					
EFB feed stock	18,360	18,360	18,360	18,360	18,360
Utility cost	188,037	184,020	183,690	184,230	184,794
Fixed O&M	3,480	3,480	3,480	3,480	3,480
Variable O&M	616	599	599	602	598
Wage of labour	16,443	16,443	16,443	16,443	16,443
Income (USD/yr)					
Power generation	117,451	114,319	114,167	114,756	114,004
Gasoline	111,219	114,154	113,396	113,876	117,152
Profit (USD/yr)	1,735	5,571	4,991	5,518	7,481
Environment					
CO_2 emission (tons CO_2/yr)	842	824	822	825	827

949
950
951
952
953
954
955
956
957
958
959
960
961
962
963
964
965
966
967
968
969
970
971

International Journal of Engineering Trends and Technology
ISSN: 2231 – 5381 /doi:10.14445/22315381/IJETT-V69I1P225

Volume 69 Issue 1, 166-171, January 2021

Development of Classification System of Rice Milling Machine Using IoT Control

B. Muangmeesri [#1], A. Theddee [*2], T. Patanasakpinyo [*3], D. Maneetham [*4]

[1] *Industrial of Technology Faculty, Valaya Alongkorn University, Thailand*

[2] *Industrial of Technology Faculty, Valaya Alongkorn University, Thailand*

[3] *Industrial of Technology Faculty, Valaya Alongkorn University, Thailand*

[4] *Department of Mechatronics Engineering, Rajamangala University of Technology Thanyaburi, Thailand*

drple2003@hotmail.com, dechrit_m@hotmail.com

Abstract *- At present, in Asia, many counties grow rice for eating and selling. But still lacking the rice milling machine used in the community. The development of this rice milling machine will focus on the development of renewable energy. Using solar energy to solar cells will be controlled by the Internet of Things (IoT) and convenience control. The result of the experiment for the theory and experiment for using an energy-saving rice milling machine. This makes it possible to save costs per household because it can use natural energy for 3 hours per day while controlling via IoT system and then can see the operation and estimates of the electrical system's use. At the same time, it can measure the value of the electric current at any time. This allows the system to be used energy efficiency and can be monitored and measured.*

Keywords: *Rice Machine, Solar Cell, Internet of Things, Automation.*

I. INTRODUCTION

The rice milling machine uses an electric motor or engine. It is a rice milling machine with a production system and a complete rice milling process. This starts with the separation of impurities first, and then the rice husks are removed using marbles or husks. By will get brown rice then rough and fine while marbles are used to get white rice then polished with a steel grid that will get white rice. The white rice may go to the rice is not white or spoiled by using the color launcher will get white rice that is more beautiful [4], [7]. Rice milling machines at present are available in many sizes according to production capacity. Which can be divided into four sizes as follows 1) community size has a production capacity of not more than 10 tons per day 2) small size with a production capacity of 10 – 40 tons per day 3) medium size with a production capacity of 40 – 100 tons per day and 4) large capacity with a production of 100 tons or more. Simultaneously, rice milling machines have to take into account the electricity-saving so as not to affect farmers or rice mill users. Because it is an electronic invention that directly converts solar energy into electrical energy. Solar cells are made from semiconductors, absorbing solar energy and converting it into electricity [2]. Where the resulting electricity is direct current, reduce the environmental impact from other forms of electricity generation such as power generation from oil or coal and promote and cultivate awareness of clean electricity production technology and the operation of the system must improve the efficiency of communication from a distance by using the control system via IoT [3]. To monitor cycle time and analyze the root cause of problems that arise both during and during the process and the continuous data collection for a long time [14]. It can also analyze working conditions very carefully.

This paper is organized as follows. In section II, the research method of the rice milling machine is presented. Solar panels, SCADA, and IoT control systems are presented in section III, and In section IV presents experimental results and conclusion.

II. RESEARCH METHOD

A. Solar Panel

This type of solar panel is made from silicon with high purity and has a long service life for the solar cells used, and the approximate size is 992*1955*35 mm. The power consumption of polycrystalline solar panel is 330 watts. The open-circuit voltage (Voc) for this solar panel is 46.20 volts, and the short circuit current (Isc) has 9.33 amps and to control the operation of the AC Motor with a size of 5 HP or 3.725 KW. So the size of the solar panel 330 wats must provide at least 16 solar panels to allow the rice milling machine to work without sunlight within 3 hours a day.

Fig 1: Solar Panel

B. Solar Panel Design

The designed system for 3.275 KW can operating Photovoltaic (PV) with the peak power system. We can be obtained a starting method.

$$P_m = (N_2 * V_m) * (N_1 * I_m) \quad (1)$$

$P_m = (N_2 * 0.85 * V_0) * (N_1 * 0.85 * I_s)$

$P_m = 3.2KW$

The module circuit current of the maximum power point (MPP), the energy consumption, and are connected parallel circuit, the total circuit voltage need to be supplied as 460 V and open circuit = 38.3 V, I_s is short circuit current = 8.96 A. Therefore,

$V_0 = 12 * 38.3 = 459.6V$

The inverter can be determined as the following equation.

$$V_{dc} = \frac{2\sqrt{2V_{LL}}}{3} \quad (2)$$

$V_{dc} = 433V$

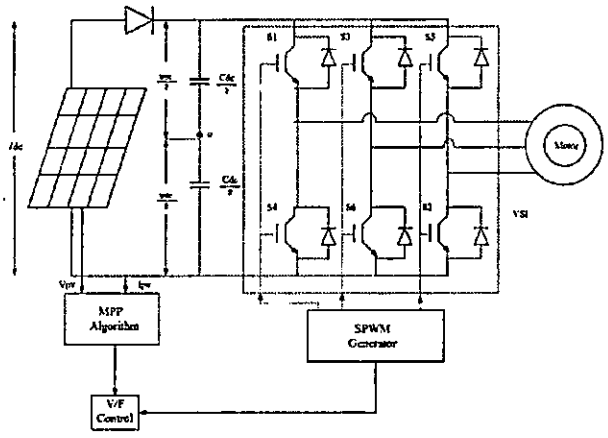

Fig 2: The designed system of PV

Calculate the value of the capacitor is:

$$C_{dc} = \frac{6 * \theta * V * I_m * t}{\left[V_{dc(ref)}^2 - V_{dc1}^2\right]} \quad (3)$$

$$C_{dc} = \frac{6 * 1.2 * 135 * 8.96 * 0.005}{\left[460^2 - 433^2\right]}$$

$C_{dc} = 1806uF$

C. Rice Mill Machine

A case study of rice milling machines has to develop and focus on building strength at the community level. Increase bargaining power in the rice market mechanism system with a suitable mill size production system, short process and efficient machinery for milling brown rice and white rice. There is softness in color, less broken. Able to preserve all the useful nutrients of rice in its entirety. This is to add the product's value to Thai rice products to maintain its leadership as a world producer of high-quality rice. It has been widely accepted that it is truly a factory and is suitable for community enterprises. This rice milling machine is designed and developed using an AC motor with 5 HP, 27 Amp current, and 1450 RPM speed. The transmission of power from the motor through the V belt. Simultaneously, all parts of the machine are connected by the transmission shaft, belt, and pulley. Able to remove rice from five channels such as white rice, brown rice, broken rice, rice husk, and chaff.

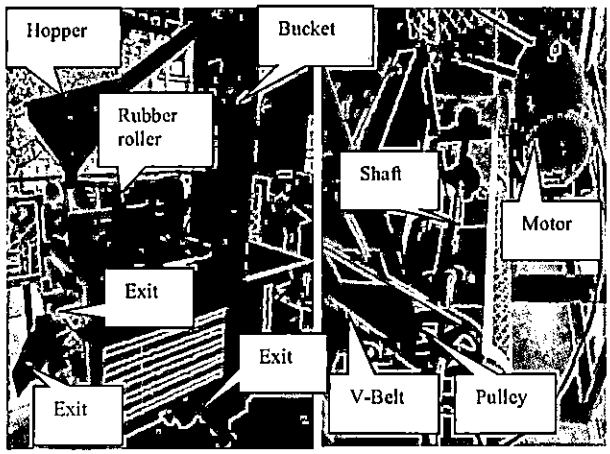

a) hopper and machine b) motor, shaft, and belt

Fig 3: Rice Milling Machine

This rice milling machine is more than 80% efficient. As shown in table 1, achieving good rice and this rice milling machine's operation can work continuously with very little impurities on the rice. The efficiency of the rice milling machine can be found as follows.

a) The rice milling machine efficiency can be obtained as:

$$M_c = \frac{W_c}{W_m} * 100$$

Where M_c = the rice milling machine Efficiency

W_c = weight of paddy in the hopper

W_m = weight of paddy outside hopper

b) The rice milling machine rate can be obtained as:

$$M_r = \frac{W_m}{T_m}$$

Where M_r = the rice milling machine rate

T_m = the rice milling machine time

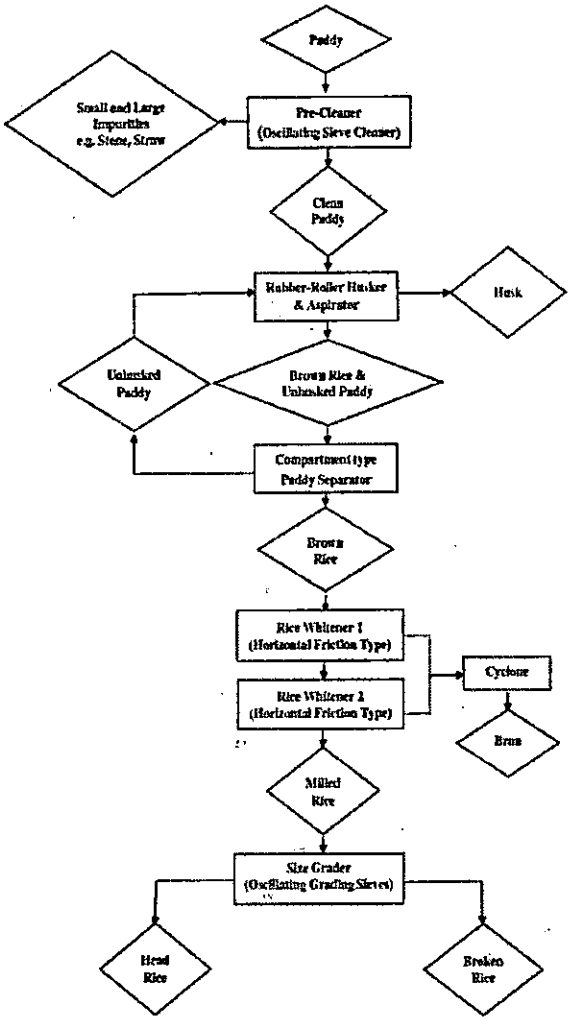

Fig 4: Flowchart of rice milling machine process

TABLE I
THE PERCENTAGE MILL AND RICE GAIN

Rice gain	Mill gain	Unmilled gain	Broken gain	Percentage mill
500	400	30	70	85
1000	650	100	250	83
1500	850	150	500	82
2000	900	300	800	80
Average	700	145	405	82.5

The rice milling machine's performance characteristics, the color of paddy can be instantly turned into milled rice, with a channel separating the chaff and bran together in one compartment. It flows through a steel sieve with a small hole filter the grits, broken rice, small pieces of rice to separate into another channel. The while level can be adjusted for various rice levels, which can be separated by the following characteristics.

1.White rice

2.Brown rice

3.Broken rice

4.Rice husk

5.Chaff

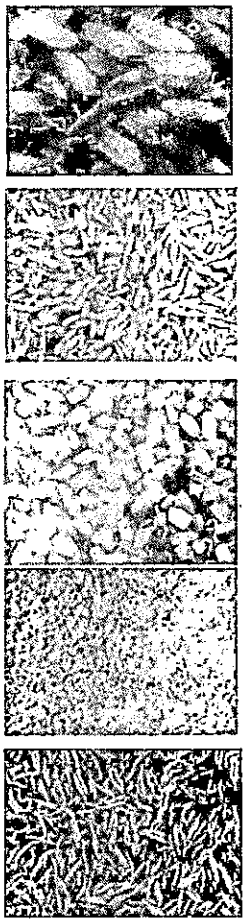

Fig 5: Type of rice

D. Battery system

When the solar panel cannot receive light such as at night, batteries are suitable for use in photovoltaic systems. Use a deep cycle battery, which is specially designed for solar cell systems. It will serve to control the charging current into the battery and increase the battery's service life. Which must be equal or greater than the current (Amp) that flows through the solar panel to the battery. In our case battery module, the charge controller's size should be larger than the solar panel's current. The capacity of the battery can be calculated as follows.

$$\text{Battery size} = \frac{c * n}{0.85 * 0.6 * Vsystem} \quad (4)$$

Where:
0.85 = power loss in battery size
0.6 = depth of discharge
V system in the voltage = 48 V
c = capacity of battery
n = working days

To calculate the daily capacity of a battery, it can be calculated as follows:

$$\text{Battery capacity to run 3 days} = \frac{\frac{3752wh}{day} * 3days}{0.85*0.6*48v}$$

$$= 459.8 \text{ Ah}$$

For the battery capacity = 120 A .

So that, battery required = 1 battery*459.8 AH/120A
= 3.8316 batteries
= 4 batteries

E. SCADA and Internet of Things

Supervisory control and data acquisition (SCADA) is a real-time monitoring and analysis system used for remote monitoring and the control of industrial control systems and various engineering systems. SCADA consists of two parts: 1) the upper-level user interface and operations 2) the SCADA remote control unit can reduce disruptions in the industrial and engineering process as the user can recognize and remotely correct incidents [15]. In addition to greatly improving work efficiency also help reduce the cost for the organization and a significant reduction in the number of people in the surveillance. By being controlled from a remote computer instead. This solar rice milling machine will be powered by a SCADA system and controlled via the Thing (IoT) system. It will use the HMS Ewon Flexy device and WebNMS IoT platform to work together to access and analyze and generate insights. The control system consists of Beckhoff PLC CPU CX9020, Flexy 205, including software that is used as a catcher, eBuddy, eWON are used as VPN client. So eWON software also away as a router and gateway for communication.

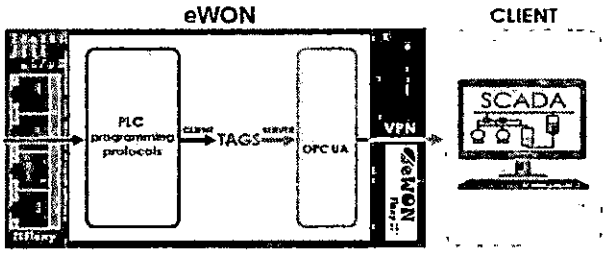

Fig 6: SCADA System

The IoT-based SCADA system will work together and manage the entire system. It improves the efficiency of the work that can monitor the system at all times and is a system that can manage, maintain, or check the voltmeter value and good electric current. In the system, analysis and visualization are the keys to building IoT applications [13]. Find basic statistical inclusions to help make decisions and make simple plans. The advanced analysis is finding relationships or the importance of insights. There is a computer program to help calculate according to various sciences such as mathematics, applied statistics, data mining, data science, etc.

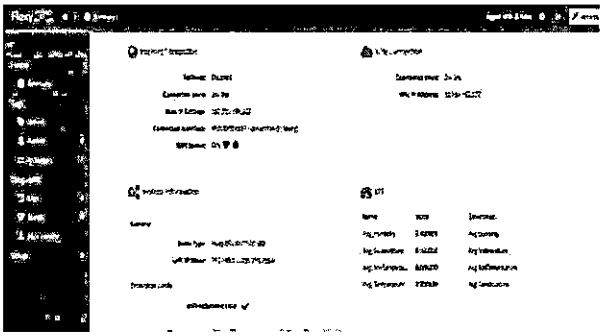

Fig 7: Flexy 205 System

Another important piece of information that should be analyzed is information about machine maintenance. We will focus on predictive maintenance, a system that monitors and analyzes data from various machine parameters. To maintain in time before the machine is broken. It is a continuous check of the parameter or various states of the machine. Users may perform more of the working behavior of machines: It has been tested to be good and accurate to indicate that the machine fails or has problems. At the same time, IoT to help display motor data and analyze operation with IoT system, ready for the rice milling machine status display. Real-time data analysis results via web browsers and can view data through other devices such as mobile phones, tablets, and so on. When machines have problems, alerts can send alert messages, get various channels, and export files in different formats.

III. EXPERIMENTAL AND RESULTS

This rice milling machine test can be controlled via a SCADA system, Modbus RTU and Modbus TCP or connected to other devices including Modbus RTU, Modbus TCP, CC-Link LON work with discrete IO to control external circuits and will receive pulse signal such as those from PLC, the counter can be used to measure and store motor power. Power consumption and the size of the load that can be used in the system.

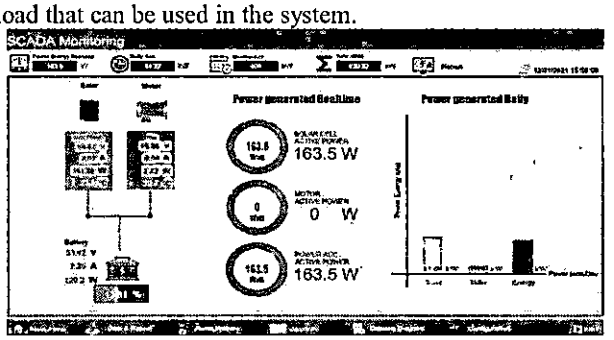

Fig 8: SCADA Monitoring

Solar panels are an innovation that is used to convert solar energy into electric energy. The resulting electric energy is direct current. Most of our home appliances tend to use AC power, and then we can convert DC electricity into AC through the inverter. The SCADA system can display results through the screen, as shown in the Figure below.

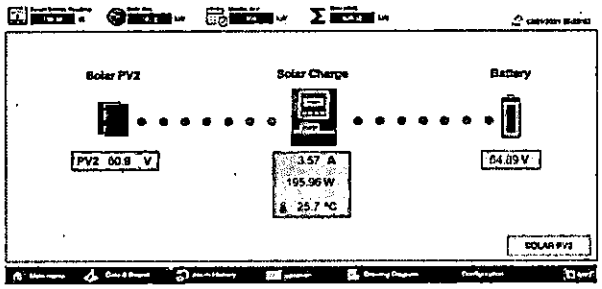

Fig 9: Solar Charge

The operation of the rice milling machine can be collected in real-time while the rice mill is used and the rice mill is not used. It can record which farmer used the rice mill at the time. How much power of the motor is used. The voltage and current are used, making it possible to promptly calculate the cost to income and expenditure and can be obtained.

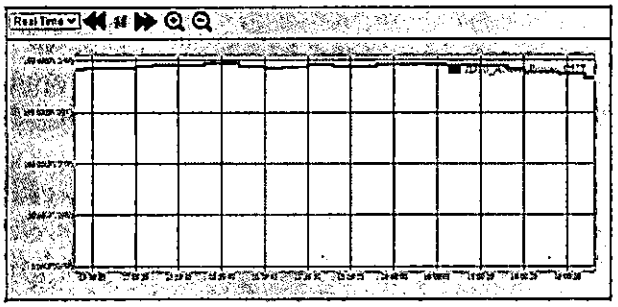

Fig 10: Shows the usage of motor

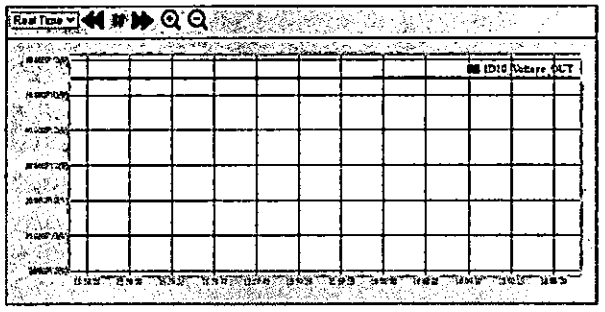

Fig 11: Shows the voltage consumption in the system

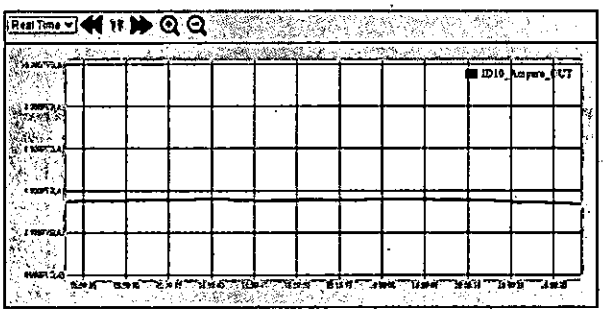

Fig12:Shows the current consumption in the system

IV. CONCLUSION

Testing this rice milling machine using solar energy controlled through a SCADA system to collect and analyze various data via a real-time monitoring system and via IoT system is a modern and fast system. The power test from solar panel to control AC motor size 3.725 KW and 27 Amp, the rice milling machine can work continuously. The values displayed by the monitor can be analyzed for various working conditions such as brightness or sunlight hardness throughout the day as well as being able to forecast the weather for how many hours the rice can be continuously milling today due to insufficient electrical system problems, it can also communicate and inform the farmers in advance. The smoothness of the electric current is very good, so it will not affect the motor system. For days without sunlight, the power system backed up on the battery can be used continuously within 1 day. For solar panels, strength, durability, and more than 10 years of solar exposure can be guaranteed.

Finally, this rice milling machine works very efficiently, and it can mill rice amount better than 82.5 %, which results in cost savings in the long run and saves farmers from the cost of milling each rice.

ACKNOWLEDGMENT

We thank the rector of Nation Innovation Agency (NIA), Thailand and The heading of the Acknowledgment section, and Valaya Alongkorn Rajabhat University for supporting the development of science and technology conditions.

REFERENCES

[1] H. Qamar, H. Qamar, and M. U. Khan, "Solar Irradiance & On Solar Power System with Net Metering in Pakistan," Advanced in Science, Technology Engineering Systems Journal, 1(2016) 1-5.

[2] S. Biswas, and A. K. Paul., A Solar Cell-based Inverter for Submersible Pumps, International Conference on Advancement in Engineering, Applied Science and Management, (2018)1-3.

[3] N. M.Tech, and B. Kunjithapathan.,Design and Implementation PV Energy System for Electrification Rural Areas., International Journal of Engineering and Advanced Technology, 8(2019).

[4] Y. Nagasaka, K. Tamaki, K. Nishiwaki, M. Saito, Y. Kikuchi, and K. Kobayashi.,Autonomous rice field operation project in NARO., International Conference on Mechatronics and Automation (IEEE), 870-874, (2011).

[5] R. F. Fernanda, M. S. Alfarisi, and P. P. Sagita., The Optimal Design in Using Solar Photovoltaic Power for SCADA to Improve System Availability: International Conference on Technology and Policy in Circuit Power and Energy, (2020).

[6] C. Hsing, and J. J. Shieh.,Solar Energy Powered Bicycle for Wireless Supervisory Control and Remote Power Management Applications., International Conference on Electrical Machine and System (IEEE), (2010) 1-4 .

[7] T. Kodama, and Y. Hata.,Development of Classification of Rice Disease Using Artificial Intelligence., International Conference on System, Man, and Cybernetics,(IEEE), 3699-3702 (2018).

[8] M. Saputra, A. Syuhada, and R. Sary.,Study of Solar Wind Energy Using as Water Pump Drive Land for Agricultural Irrigation., International Conference on Science and Technology (IEEE), (2010) 1-4.

[9] M.R.S Muthusinghe, S.T. Palliyaguru, W.A.N.D. Weerakkody, A.M. H. Saranga, and W.H Rankothge, Towards Smart Farming: Accurate Prediction of Paddy Harvest and Rice Demand., International Conference on Humanitarian Technology (IEEE), (2018) 1-6.

[10] H. Min, S. Shuang, X. X. Bing, C. F. Bo, and Z. Y. Bin.,Why high grain yield can be achieved in single seedling machine transplanted

hybrid rice under dense planting conditions, Journal of Integrative Agriculture, 17(6)(2018) 1299-1306.

[11] H. Terzioglu, and F. A. Kazan., The Designing of a Wducational Solar Panel That can be Controlled in Different Ways., International Conference on Information Science and Control Engineering, (IEEE), (2015) 960-964.

[12] R. J. Tom, and S. Sankaranarayanan.,IoT based SCADSA Integrated with for Power Distribution Automation," International Conference on Information Systems and Technologies, (IEEE)(2017) 1-4.

[13] M. Zamanlou, and M. T. Iqbal.,Development of an Economical SCADA System for Solar Water Pumping in Iran," International Conference on IoT, Electronics, Mechatronics, (IEEE), 1-4(2020).

[14] R. Dugyala, N, H. Reddy, and S. Kumar.,Implementation of SCADA Through Cloud-Based IoT Decices- Initial Design Steps., International Conference of Cloud Computing with the Internet of Things, (IEEE)(2019) 1-6.

[15] L. O. Aghenta, and M. T. IqbalN., Development of an IoT Based Open Source SCADA System for PV System Monitoring., International Conference of Electrical and Computer Engineering, (IEEE), 1-4(2019).

[16] K. Medrano, D. Altuve, K. Belloso, and C. Bran., Development of SCADA using an RTU based on IoT controller..International Conference on Automatica, (IEEE)(2018) 1-6.